

Competing orders in the generalized Hund chain model at half filling

H. Nonne,¹ E. Boulat,² S. Capponi,^{3,4} and P. Lecheminant¹

¹Laboratoire de Physique Théorique et Modélisation, CNRS UMR 8089, Université de Cergy-Pontoise, Site de Saint-Martin, F-95300 Cergy-Pontoise Cedex, France

²Laboratoire Matériaux et Phénomènes Quantiques, Université Paris Diderot, 2 Place Jussieu, 75205 Paris Cedex 13, France

³Laboratoire de Physique Théorique, IRSAMC, Université de Toulouse–UPS, F-31062 Toulouse, France

⁴LPT, IRSAMC, CNRS, F-31062 Toulouse, France

(Received 28 June 2010; published 22 October 2010; publisher error corrected 24 November 2010)

By using a combination of several nonperturbative techniques—a one-dimensional field theoretical approach together with numerical simulations using density-matrix renormalization group—we present an extensive study of the phase diagram of the generalized Hund model at half filling. This model encloses the physics of various strongly correlated one-dimensional systems, such as two-leg electronic ladders, ultracold degenerate fermionic gases carrying a large hyperfine spin $\frac{3}{2}$, other cold gases such as ytterbium 171 or alkaline-earth condensates. A particular emphasis is laid on the possibility to enumerate and exhaust the eight possible Mott-insulating phases by means of a duality approach. We exhibit a one-to-one correspondence between these phases and those of the two-leg electronic ladders with interchain hopping. Our results obtained from a weak-coupling analysis are in remarkable quantitative agreement with our numerical results carried out at moderate coupling.

DOI: [10.1103/PhysRevB.82.155134](https://doi.org/10.1103/PhysRevB.82.155134)

PACS number(s): 71.10.Pm, 71.10.Fd

I. INTRODUCTION

A major focus of the study of strongly correlated electronic systems is the analysis of the competition between qualitatively distinct ground states and the associated quantum phase transitions (QPTs) (Ref. 1) in low dimensions. A reason to concentrate on these matters stems from the hope that the criticality of the system at such QPTs possibly results in a universal description of their vicinity. In 2+1 space-time dimensions, the resulting relativistic quantum field theories which describe the zero-temperature transition between these quantum phases are in general strongly coupled and can be highly nontrivial.²

In one dimension (1D), the situation is much simpler since the quantum critical points in standard condensed-matter systems are characterized by conformal field theories (CFTs), which often admit a simple free-field representation in terms of free bosons or fermions. In this respect, the bosonization approach has been very successful to investigate the physical properties of one-dimensional quantum phases.^{3,4} Within this approach, several conventional and exotic long-range-ordered phases have been revealed over the years in two-leg ladder models^{5–18} and carbon nanotube systems^{19–22} at half filling. Two different classes of Mott-insulating phases have been found at half filling in these systems. A first class is twofold degenerate corresponding to the spontaneous breaking of discrete symmetries such as the translation symmetry in charge-density wave (CDW) and bond-ordering phases, or the time-reversal symmetry in d-density wave (DDW) phase. In contrast, the second class of Mott-insulating phases is nondegenerate. A paradigmatic example of this class is the Haldane phase of the spin-1 Heisenberg chain²³ and of the two-leg spin ladder which breaks spontaneously a nonlocal $Z_2 \times Z_2$ discrete symmetry.^{24–26}

Another striking particularity of many one-dimensional electronic systems is the existence of hidden duality symmetries, within the low-energy approach, which relate many of the competing orders to a conventional one like the CDW.^{5,13,27–31} Actually, a general duality approach has been introduced recently to describe the zero-temperature spin-gapped phases of 1D electronic systems away from half filling.³¹ In this paper, we apply this approach to half-filled systems of four-component fermions and revisit the problem of competing orders in half-filled two-leg electronic ladders. In this particular case, some of the duality symmetries already exist at the level of the lattice model, and have been first revealed in Ref. 13. In addition to these, as it will be seen, there are also interesting *emergent duality symmetries* which relate nondegenerate Mott-insulating phases to conventional order such as CDW. Unlike the former ones, those dualities do not bear a local representation on the lattice.

The starting point of the duality approach to competing orders is to identify the internal global symmetry group H of the lattice model. For two-leg electronic ladders, or more generally two-band models, the building blocks of the model are four-component fermionic creation operators on each site i : $c_{l\sigma,i}^\dagger$ where $l=1,2$ is the leg or orbital index and $\sigma=\uparrow,\downarrow$ denotes the spin- $\frac{1}{2}$ index. Three basic global continuous symmetries are retained: a U(1) charge symmetry ($c_{l\sigma,i} \rightarrow e^{i\phi} c_{l\sigma,i}$), a SU(2) spin-rotational invariance [$c_{l\sigma,i} \rightarrow \sum_{\sigma'} (e^{i\vec{\theta} \cdot \vec{\sigma}/2})_{\sigma\sigma'} c_{l\sigma',i}$, $\vec{\sigma}$ being the Pauli matrices], and a U(1) orbital symmetry ($c_{1(2)\sigma,i} \rightarrow e^{\pm i\phi} c_{1(2)\sigma,i}$). Moreover, we will consider models for which the two legs or two bands behave identically; in other words, we impose a Z_2 invariance under the permutation of the legs. If we restrict ourselves to on-site interactions, the most general model with $H=U(1)_c \times SU(2)_s \times U(1)_o \times Z_2$ invariance then reads as follows:³²

$$\begin{aligned} \mathcal{H} = & -t \sum_{i,l\sigma} (c_{l\sigma,i}^\dagger c_{l\sigma,i+1} + \text{H.c.}) - \mu \sum_i n_i + \frac{U}{2} \sum_i n_i^2 \\ & + J_H \sum_i \vec{S}_{1,i} \cdot \vec{S}_{2,i} + J_l \sum_i (T_i^z)^2 \end{aligned} \quad (1)$$

with $n_i = \sum_{l\sigma} n_{l\sigma,i}$ ($n_{l\sigma,i} = c_{l\sigma,i}^\dagger c_{l\sigma,i}$) being the occupation number on the i th site. In Eq. (1), the spin operator on leg l is defined by

$$\vec{S}_{l,i} = \frac{1}{2} \sum_{\alpha,\beta} c_{l\alpha,i}^\dagger \vec{\sigma}_{\alpha\beta} c_{l\beta,i} \quad (2)$$

whereas $T_i^z = \frac{1}{2} \sum_{\sigma} (n_{1\sigma,i} - n_{2\sigma,i})$ is the generator of the U(1) symmetry for orbital degrees of freedom.

Model (1) depends on three microscopic couplings: a Coulombic interaction U , a Hund coupling J_H , and an ‘‘orbital crystal-field anisotropy’’ J_l . When $J_l=0$, the resulting model is the so-called Hund model which has been investigated in the context of orbital degeneracy.^{15,28,32} The generalized Hund model (1) is directly linked to ultracold fermionic ¹⁷¹Yb and alkaline-earth atoms with nuclear spin $I=\frac{1}{2}$.^{33,34} The two-orbital states are described in these systems by the ground state (¹S₀ ≡ g) and a long-lived excited state (³P₀ ≡ e). The almost perfect decoupling of the nuclear spin from the electronic angular momentum J in the two e, g states ($J=0$ states) makes the s -wave scattering lengths of the problem independent of the nuclear spin. The low-energy Hamiltonian relevant to the ¹⁷¹Yb cold gas loaded into a 1D optical lattice then reads³⁴

$$\begin{aligned} \mathcal{H}_{\text{Yb}} = & -t \sum_{i,l\sigma} (c_{l\sigma,i}^\dagger c_{l\sigma,i+1} + \text{H.c.}) + \frac{\tilde{U}}{2} \sum_{i,l} n_{l,i} (n_{l,i} - 1) \\ & + V \sum_i n_{g,i} n_{e,i} + V_{ex} \sum_{i,\alpha,\beta} c_{g\alpha,i}^\dagger c_{e\beta,i}^\dagger c_{g\beta,i} c_{e\alpha,i}, \end{aligned} \quad (3)$$

where $c_{l\sigma,i}^\dagger$ is the fermionic creation operator at site i with the nuclear spin- $\frac{1}{2}$ index $\sigma = \uparrow, \downarrow$ in the $l=e, g$ electronic states. The occupation number of electronic states is $n_{l,i} = \sum_{\sigma} c_{l\sigma,i}^\dagger c_{l\sigma,i}$. Model (3) is then directly equivalent to the generalized Hund model (1) with the correspondence: $\tilde{U}=U+J_l/2$, $V=U-J_l/2-J_H/4$, and $V_{ex}=-J_H/2$.

Apart from this connection to cold fermions physics, one of the main interests of model (1) stems from the fact that it contains a large variety of relevant models with extended continuous symmetries, some of which having appeared in different contexts. First of all, when $J_l=-3J_H/4$, the continuous symmetry is promoted to U(1)_c × SU(2)_s × SU(2)_o, and one recovers the so-called spin-orbital model.^{35–39} In absence of Hund coupling, i.e., $J_H=0$, the continuous symmetry group of model (1) is U(1)_c × U(1)_o × SO(4)_s where each chain has a separate SU(2) spin-rotational symmetry. When $J_l=J_H/4$, model (1) displays an SO(5) symmetry which unifies spin and orbital degrees of freedom. The resulting model, with U(1)_c × SO(5)_{s,o} continuous symmetry, is relevant to four-component fermionic cold atom systems.^{40–50} Finally, when $J_H=J_l=0$, one recovers the U(4) Hubbard model, that has been extensively analyzed in recent years.^{14,51–53} As it will be seen in Sec. II, at half filling, many

other highly symmetric lines can be identified. For instance, the line $J_H=8U$ unifies spin and charge degrees of freedom with an extended U(1)_o × SO(5)_{s,c} continuous symmetry.⁵⁴ The corresponding model has been previously introduced by Scalapino, Zhang, and Hanke (SZH) (Ref. 6) in connection to the SO(5) theory which relates antiferromagnetism to d -wave superconductivity.⁵⁵

In this paper, we will investigate the nature of the insulating phases of the zero-temperature phase diagram of model (1) at half filling. In this respect, it will be shown that the duality approach of Ref. 31 for half-filled fermions with internal global symmetry group $H=U(1)_c \times SU(2)_s \times U(1)_o \times Z_2$ yields eight fully gapped phases. These eight Mott-insulating phases fall into two different classes. On one hand, the first class consists of four doubly degenerate phases which spontaneously break a discrete symmetry of the underlying lattice model. On the other hand, the second class contains four nondegenerate Mott-insulating phases. A first one is the rung-singlet (RS) phase where two spins on each rung lock into a singlet. A second nondegenerate phase is a rung-triplet (RT) phase where the spins now combine into a triplet and this phase is known to be adiabatically connected to the Haldane phase of the spin-1 Heisenberg chain.²⁶ Finally, two other Haldane-type phases are found: they are spin singlet but involve two different pseudospin-1 operators which are, respectively, built from charge and orbital degrees of freedom. In the case of the charge pseudospin-1 operator, the resulting Haldane charge (HC) phase has been found very recently in the context of 1D half-filled spin- $\frac{3}{2}$ cold fermions.⁵⁰

In addition to this duality approach, it will be shown, by means of a one-loop renormalization group (RG) approach and numerical simulations [using the density-matrix renormalization group (DMRG) algorithm⁵⁶], that the zero-temperature phase diagram of model (1) displays seven out of the eight expected insulating phases. We find it remarkable that model (1), that only has three independent coupling constants, turns out to have a rich phase diagram which includes the four nondegenerate Mott-insulating phases.

Finally, we will make contact with the eight Mott-insulating phases found over the years in half-filled generalized two-leg ladders with a t_\perp transverse hopping term.^{11,12} The latter term breaks explicitly the U(1)_o symmetry but it is known that this symmetry is recovered at low energy.^{5,12} The relevant global symmetry group is still H and the same duality approach thus applies to that case. In this respect, we will connect the two families of eight fully gapped phases found for $t_\perp=0$ and for $t_\perp \neq 0$. In particular, it will be shown that the two problems are in fact connected by an emergent nonlocal duality symmetry.

The rest of the paper is organized as follows. In Sec. II, we discuss the symmetries of model (1). We also present a strong-coupling analysis along special highly symmetric lines which gives some clues about the nature of the nondegenerate Mott-insulating phases. The low-energy investigation is then presented in Sec. III. It contains the duality approach to half-filled fermions with internal symmetry group $H=U(1)_c \times SU(2)_s \times U(1)_o \times Z_2$. The zero-temperature phase diagram of the generalized Hund model (1) and that of highly symmetric models are deduced by a one-loop RG

analysis. We then connect our results to the known insulating phases of generalized two-leg ladder models with a t_\perp hopping term. In Sec. IV, we map out the phase diagram of model (1), SZH, and spin-orbital models with $t_\perp=0$ by means of DMRG calculations to complement the low-energy approach. Our concluding remarks are presented in Sec. V. The paper is supplied with three appendices which provide some additional information. Appendix A describes the technical details of the continuum limit of model (1). The low-energy approach of edge states in the nondegenerate Mott-insulating phases are discussed in Appendix B. Finally, Appendix C presents the main effect of the interchain hopping in the strong-coupling regime, close to the orbital symmetric line.

II. SYMMETRIES AND STRONG COUPLING

Before investigating the zero-temperature phase diagram of the generalized Hund model by means of the low-energy and DMRG approaches, it is important to fully determine the special lines which exhibit enlarged symmetry. It turns out that, at half filling, many highly symmetric lines can be highlighted. Their study will give some important clues on the possible Mott-insulating phases of the model at half filling.

A. Highly symmetric lines

The generalized Hund model (1) enjoys a global internal symmetry group $H=U(1)_c \times SU(2)_s \times U(1)_o \times Z_2$ on top of the lattice discrete symmetries such as one-step translation invariance, time-reversal symmetry, site and link parities. For generic filling, and on four different manifolds—that correspond to some fine tuning of the lattice couplings—in the space of coupling constants, this model possesses a higher symmetry.

First of all, on top of the $SU(2)_s$ that rotates spin degrees of freedom, one can define a $SU(2)_o$ orbital pseudospin operator,

$$T_i^\dagger = c_{1\uparrow,i}^\dagger c_{2\uparrow,i} + c_{1\downarrow,i}^\dagger c_{2\downarrow,i},$$

$$T_i^c = \frac{1}{2}(n_{1,i} - n_{2,i}) \quad (4)$$

with $n_{l,i} = \sum_\sigma n_{l\sigma,i}$, $l=1,2$. When $J_i = -3J_H/4$, the $U(1)$ orbital symmetry of the Hund model (1) is enlarged to $SU(2)_o$, with generators given by Eq. (4). The resulting model displays a $U(1)_c \times SU(2)_s \times SU(2)_o$ continuous symmetry and has been considered in systems with orbital degeneracy like the spin-orbital model.^{32,35–39}

A second highly symmetric model is defined for $J_H=0$: then the interacting part of model (1) simplifies as follows:

$$\mathcal{H}_{\text{SO}(4)}^{\text{int}} = \frac{1}{2} \left(U + \frac{J_t}{2} \right) \sum_i (n_{1,i}^2 + n_{2,i}^2) + \left(U - \frac{J_t}{2} \right) \sum_i n_{1,i} n_{2,i}, \quad (5)$$

from which we deduce that each leg has a separate $SU(2)$ spin rotation symmetry so that the continuous symmetry group of model (5) is $U(1)_c \times U(1)_o \times \text{SO}(4)_s$.

When $J_i = J_H/4$, as shown in Ref. 54, model (1) is known to be equivalent to the spin- $\frac{3}{2}$ cold fermionic model with interacting part,

$$\mathcal{H}_{\text{spin-3/2}}^{\text{int}} = U_0 \sum_i P_{00,i}^\dagger P_{00,i} + U_2 \sum_i \sum_{m=-2}^2 P_{2m,i}^\dagger P_{2m,i}, \quad (6)$$

where $U_0 = (2U - 7J_t)/4$ and $U_2 = (2U + J_t)/4$. In Eq. (6), we have $P_{Jm,i}^\dagger = \sum_{\alpha\beta} \langle Jm | \frac{3}{2}, \frac{3}{2}; \alpha\beta \rangle c_{\alpha,i}^\dagger c_{\beta,i}^\dagger$, $\alpha, \beta = \pm \frac{3}{2}, \pm \frac{1}{2}$, and $\langle Jm | \frac{3}{2}, \frac{3}{2}; \alpha\beta \rangle$ are the Clebsch-Gordan coefficients for spin $\frac{3}{2}$. Model (6) is known to exhibit a $U(1)_c \times \text{SO}(5)_{s,o}$ continuous symmetry without any fine tuning.⁴⁰

Finally, for $J_H = J_t = 0$, spin and orbital degrees of freedom unify to a maximal $SU(4)$ symmetry and model (1) takes the form of the Hubbard model for four component fermions with a $U(4)$ invariance.

At half filling, the chemical potential μ is given by $\mu_0 = \frac{3U}{2}$ to ensure particle-hole symmetry. More highly symmetric lines can be found in this particle-hole symmetric case. It stems from the fact that, as in the spin- $\frac{1}{2}$ Hubbard model, the $U(1)_c$ charge symmetry can be enlarged to an $SU(2)_c$ symmetry at half filling.^{57,58} In this respect, one can define a charge pseudospin operator by

$$J_i^\dagger = c_{1\uparrow,i}^\dagger c_{2\downarrow,i}^\dagger - c_{1\downarrow,i}^\dagger c_{2\uparrow,i}^\dagger,$$

$$J_i^c = \frac{1}{2}(n_i - 2), \quad (7)$$

which is a $SU(2)_s$ spin singlet that satisfies the $SU(2)$ commutation relations. This operator is the generalization in two-leg ladder or two-band systems of the pseudospin- $\frac{1}{2}$ operator introduced by Anderson⁵⁹ and by Yang in η -pairing problems.⁵⁷

Many interesting lines can then be considered. A simple way to reveal them is to consider the energy levels of the one-site Hamiltonian (1) with $t=0$. The corresponding spectrum is depicted in Fig. 1. On top of the four symmetric lines that we have identified above, we find nine additional lines where higher continuous symmetries emerge (see Table I). Among all these new highly symmetric lines, there are three interesting models with two independent coupling constants, i.e., with only one fine tuning.

A first one corresponds to the SZH model with $U(1)_o \times \text{SO}(5)$ continuous symmetry. Such SZH model with no transversal hopping t_\perp is defined as follows: $\mathcal{H}_{\text{SZH}} = \mathcal{H}_{t_\parallel} + \mathcal{H}_{\text{rung}}$ with

$$\mathcal{H}_{t_\parallel} = -t \sum_{i,\sigma} (c_{\sigma,i}^\dagger c_{\sigma,i+1} + d_{\sigma,i}^\dagger d_{\sigma,i+1} + \text{H.c.}),$$

$$\mathcal{H}_{\text{rung}} = U_{\text{SZH}} \sum_i \left[\left(n_{c\uparrow,i} - \frac{1}{2} \right) \left(n_{c\downarrow,i} - \frac{1}{2} \right) + (c \rightarrow d) \right]$$

$$+ V_{\text{SZH}} \sum_i (n_{c,i} - 1)(n_{d,i} - 1) + J_{\text{SZH}} \sum_i \vec{S}_{c,i} \cdot \vec{S}_{d,i}, \quad (8)$$

where c_σ and d_σ are, respectively, the fermion annihilation operator of the upper and lower leg of the ladder with spin

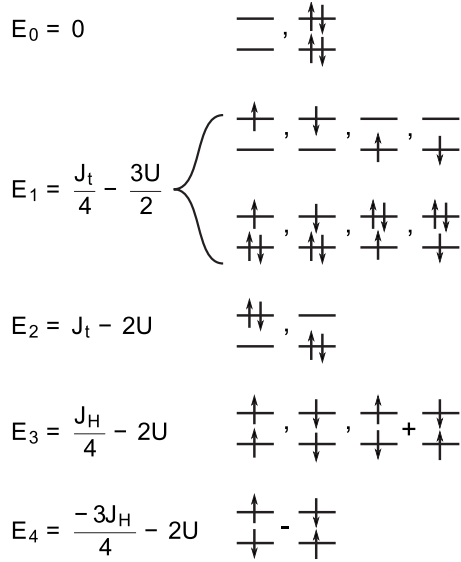


FIG. 1. Energy-level diagram for the one-site Hamiltonian (1) with $t=0$.

index σ . The occupation numbers on the i th site are denoted by $n_{c(d),i}$, respectively. The spin operators $\vec{S}_{c(d),i}$ are defined similarly to those of the Hund model [see Eq. (2)]. It is straightforward to relate the SZH model to the generalized Hund model (1),

$$U = \frac{U_{\text{SZH}} + V_{\text{SZH}}}{2},$$

$$J_H = J_{\text{SZH}},$$

$$J_t = U_{\text{SZH}} - V_{\text{SZH}}. \quad (9)$$

As shown in Ref. 6, the fine tuning $J_{\text{SZH}}=4(U_{\text{SZH}}+V_{\text{SZH}})$ [i.e., $J_H=8U$ in the context of model (1)] makes the lattice model (8) $U(1)_o \times \text{SO}(5)_{s,c}$ symmetric. The $\text{SO}(5)$ symmetry unifies here spin and charge degrees of freedom and is thus

different from the spin- $\frac{3}{2}$ cold fermionic atoms [Eq. (6)] case.

A second symmetric line is found for $J_t=2U$ with the emergence of a $\text{SU}(2)_s \times \text{SO}(4)_{c,o}$ continuous symmetry. In that case, charge and orbital degrees of freedom play a symmetric role and are unified by a $\text{SO}(4)$ symmetry.

Finally, the last extended symmetric ray with the fine tuning $J_H=-8U/3$ (see Table I) corresponds to a model with $U(1)_o \times \text{SU}(2)_c \times \text{SU}(2)_s$ continuous symmetry. Such a model has two independent $\text{SU}(2)$ symmetries: one for the spin degrees of freedom and also a second for the charge degrees of freedom. In this respect, it is very similar to the spin-orbital model and can be called “charge-spin” model.

B. Strong-coupling analysis

The identification of these highly symmetric models is very useful since several possible insulating phases of the generalized Hund model (1) can be inferred from a strong-coupling analysis. Such an approach has already been performed for some special lines of Table I such as the half-filled $U(4)$ Hubbard chain,^{60,61} the $\text{SO}(5)$ spin- $\frac{3}{2}$ model,^{45,50} and the SZH one.^{6,7}

Here, we present a simple strong-coupling approach along three special lines which enables us to identify several non-degenerate Mott-insulating phases. To this end, let us first consider the line $J_t=2U$ with $U>0$ and $J_H<0$. In the absence of hopping term (i.e., $t=0$), the lowest-energy states are the spin triplet E_3 (see Fig. 1). An effective Hamiltonian can then be deduced by treating the hopping term as a perturbation in the strong-coupling regime $|U, J_H, J_t| \gg t$. At second order of perturbation theory, we find an antiferromagnetic $\text{SU}(2)$ Heisenberg chain,

$$\mathcal{H}_{\text{eff}} = J_s \sum_i (\vec{S}_{1,i} + \vec{S}_{2,i}) \cdot (\vec{S}_{1,i+1} + \vec{S}_{2,i+1}), \quad (10)$$

where $J_s = -4t^2/(J_H - 4U) > 0$, and $\vec{S}_{l,i}$ are the spin operators defined in Eq. (2). The resulting fully gapped phase is the well-known RT phase of the two-leg spin- $\frac{1}{2}$ ladder which is adiabatically connected to the Haldane phase of the spin-1

TABLE I. Extended continuous symmetries of model (1) at half filling.

Extended continuous symmetry	Fine tuning	Degenerate levels
$U(1)_c \times \text{SU}(2)_o \times \text{SU}(2)_s$	$J_t = -3J_H/4$	$E_2 = E_4$
$U(1)_c \times U(1)_o \times \text{SO}(4)_s$	$J_H = 0$	$E_3 = E_4$
$U(1)_c \times \text{SO}(5)_{s,o}$	$J_t = J_H/4$	$E_2 = E_3$
$U(1)_c \times \text{SU}(4)_{s,o}$	$J_H = J_t = 0$	$E_2 = E_3 = E_4$
$\text{SO}(7)$	$J_t = 2U, J_H = 8U$	$E_0 = E_2 = E_3$
$U(1)_o \times \text{SU}(4)_{s,c}$	$U = J_H = 0$	$E_0 = E_3 = E_4$
$\text{SU}(2)_c \times \text{SO}(5)_{s,o}$	$J_t = -2U/3, J_H = -8U/3$	$E_0 = E_4, E_2 = E_3$
$\text{SU}(2)_o \times \text{SO}(5)_{s,c}$	$J_t = -6U, J_H = 8U$	$E_0 = E_3, E_2 = E_4$
$\text{SO}(5)_{c,o} \times \text{SU}(2)_s$	$J_t = 2U, J_H = -8U/3$	$E_0 = E_2 = E_4$
$U(1)_o \times \text{SO}(5)_{s,c}$	$J_H = 8U$	$E_0 = E_3$
$\text{SO}(4)_{c,o} \times \text{SO}(4)_s$	$J_H = 0, J_t = 2U$	$E_0 = E_2, E_3 = E_4$
$\text{SO}(4)_{c,o} \times \text{SU}(2)_s$	$J_t = 2U$	$E_0 = E_2$
$U(1)_o \times \text{SU}(2)_s \times \text{SU}(2)_c$	$J_H = -8U/3$	$E_0 = E_4$

chain.²⁶ Such a nondegenerate gapful phase displays a hidden antiferromagnetic ordering which is revealed by a string-order parameter,^{25,62,63}

$$\lim_{|i-j| \rightarrow \infty} \langle (S_{1,i}^z + S_{2,i}^z) e^{i\pi \sum_{k=i+1}^{j-1} (S_{1,k}^z + S_{2,k}^z)} (S_{1,j}^z + S_{2,j}^z) \rangle \neq 0. \quad (11)$$

This RT phase is also known to exhibit spin- $\frac{1}{2}$ edge states when open-boundary conditions (OBCs) are considered.^{64–66}

A second interesting line is $J_H = -8U/3$ where the charge degrees of freedom enjoy an SU(2) symmetry enlargement. In the absence of hopping term, the lowest-energy states for $U < 0$ and $J_t > 0$ are the E_0, E_4 levels as it can be seen from Fig. 1. Keeping only these three states, we obtain, at second order of perturbation theory, an effective (pseudo) spin-1 antiferromagnetic SU(2) Heisenberg chain,

$$\mathcal{H}_{\text{eff}} = J_c \sum_i \vec{J}_i \cdot \vec{J}_{i+1} \quad (12)$$

with $J_c = -4t^2/(6U - J_t) > 0$. The effective Hamiltonian (12) expresses in terms of the spin-singlet charge operator (7) which is a pseudospin-1 operator in the triplet states E_0, E_4 of Fig. 1. We then expect the emergence of Haldane-type phase for charge degrees of freedom as it has been recently found in the context of half-filled spin- $\frac{3}{2}$ cold fermions.⁵⁰ Such a HC phase is fully gapped and nondegenerate. It displays a hidden ordering that is revealed by the string-order parameter,

$$\lim_{|i-j| \rightarrow \infty} \langle J_i^z e^{i\pi \sum_{k=i+1}^{j-1} J_k^z} \rangle \neq 0. \quad (13)$$

A deviation from the line $J_H = -8U/3$ breaks the SU(2) charge symmetry down to U(1) and in the strong-coupling regime the lowest correction to model (12) is a single-ion anisotropy term $D_c \sum_i (J_i^z)^2$ (with $D_c = 3J_H/4 + 2U$). The Haldane phase of the spin-1 chain is known to be stable under a weak single-ion anisotropy.⁶⁷ A large enough D_c may give rise to a Ising phase with $\langle J_i^z \rangle \neq 0$ [i.e., a CDW from definition (7)] or to a large- D_c phase which is a nondegenerate gapped singlet phase. The latter, with $\langle J_i^z \rangle = 0$, corresponds to the RS phase of the two-leg spin- $\frac{1}{2}$ ladder where the two spins of the rung bind into a singlet state (E_4 state of Fig. 1) for an antiferromagnetic interchain coupling.

Finally, a last interesting symmetric ray is $J_t = -3J_H/4$ where the U(1) orbital symmetry is enlarged to SU(2). Along this line, when $J_H > 0$ and U is not too negative, the lowest-energy states of the one-site Hamiltonian are levels E_2, E_4 of Fig. 1. At second order of perturbation theory, we now find a spin-1 antiferromagnetic SU(2) Heisenberg chain for the orbital degrees of freedom,

$$\mathcal{H}_{\text{eff}} = J_o \sum_i \vec{T}_i \cdot \vec{T}_{i+1} \quad (14)$$

with $J_o = 16t^2/(9J_H + 8U)$. We thus expect the emergence of a new Haldane phase for the orbital degrees of freedom that will be called Haldane orbital (HO) phase in the rest of the paper. The resulting hidden ordering is captured by the following string-order parameter:

$$\lim_{|i-j| \rightarrow \infty} \langle T_i^z e^{i\pi \sum_{k=i+1}^{j-1} T_k^z} \rangle \neq 0. \quad (15)$$

A deviation from the line $J_t = -3J_H/4$ breaks the SU(2) orbital symmetry down to U(1) and in the strong-coupling regime the lowest correction to model (14) is a single-ion anisotropy term $D_o \sum_i (T_i^z)^2$ (with $D_o = J_t + 3J_H/4$). For sufficiently strong value of $|D_o|$, the HO phase will be destabilized into either an orbital density wave (ODW) which is described by the E_2 states with $\langle T_i^z \rangle \neq 0$ or a RS phase, i.e., the E_4 state with $\langle T_i^z \rangle = 0$.

In summary, the strong-coupling analysis along highly symmetric lines reveals the existence of four nondegenerate Mott-insulating phases (RT, HC, HO, and RS) and two gapful phases with long-range density ordering (CDW and ODW).

III. LOW-ENERGY APPROACH

In this section, we present the details of the low-energy approach of the generalized Hund model (1) at half filling, in the weak-coupling regime $|U, J_H, J_t| \ll t$. The zero-temperature phase diagram of model (1) will be investigated by means of the combination of a duality approach and one-loop RG calculations. In particular, we will determine the different insulating phases in the weak-coupling regime and make connection with the ones found within the strong-coupling approach.

A. Phenomenological approach

The starting point of the low-energy approach is the linearization around the Fermi points $\pm k_F$ of the dispersion relation for noninteracting four-component fermions. We thus introduce four left- and right-moving Dirac fermions $L_{l\sigma}, R_{l\sigma}$ ($l=1, 2$ and $\sigma=\uparrow, \downarrow$), which describe the lattice fermions $c_{l\sigma,i}$ in the continuum limit,

$$\frac{c_{l\sigma,i}}{\sqrt{a_0}} \rightarrow R_{l\sigma}(x) e^{ik_F x} + L_{l\sigma}(x) e^{-ik_F x} \quad (16)$$

with $k_F = \pi/2a_0$ at half filling and $x = ia_0$ (a_0 being the lattice spacing). The next step of the approach is to use the Abelian bosonization of these Dirac fermions to obtain the low-energy effective Hamiltonian for model (1). The details of these calculations are given in Appendix A. Here, we present a more phenomenological approach which is based on the symmetries of the lattice model (1).

The continuous symmetry of the noninteracting model (1) is SO(8). In the continuum limit, the SO(8) symmetry can be revealed by introducing eight real (Majorana) fermions from the four complex Dirac $(R, L)_{l\sigma}$ ones. The noninteracting fixed point is then described by the SO(8)₁ CFT with central charge $c=4$.⁶⁸ The chiral currents $J_{L,R}^{(a,b)}$ ($1 \leq a < b \leq 8$), which generates this CFT, can be expressed as fermionic bilinears: $J_{L(R)}^{(a,b)} = i \xi_{L(R)}^a \xi_{L(R)}^b$, where $\xi_{L(R)}^a$ are the eight left- (right-) moving Majorana fermions.

When interactions are included, the SO(8) symmetry is broken down to $H = U(1)_c \times SU(2)_s \times U(1)_o \times Z_2$. The key point of the analysis is to identify how the eight Majorana

fermions of the $SO(8)_1$ CFT act in H . One way to obtain the correspondence is to focus on the currents which generate the different continuous symmetry groups in H . The uniform part of the continuum limit of the spin operator (2) on the leg $l=1,2$ defines the chiral $SU(2)_1$ currents $\vec{J}_{lR,L}$,

$$\vec{J}_{lL} = L_{l\alpha}^\dagger \frac{\vec{\sigma}_{\alpha\beta}}{2} L_{l\beta}, \quad \vec{J}_{lR} = R_{l\alpha}^\dagger \frac{\vec{\sigma}_{\alpha\beta}}{2} R_{l\beta}. \quad (17)$$

As in two-leg spin ladder,^{25,69} the sum and difference of these chiral $SU(2)_1$ currents can be locally expressed in terms of four Majorana fermions $\xi_{R,L}^{1,2,3,6}$ among the eight original ones,

$$\begin{aligned} \vec{J}_{1R,L} + \vec{J}_{2R,L} &= -\frac{i}{2} \vec{\xi}_{R,L} \wedge \vec{\xi}_{R,L}, \\ \vec{J}_{1R,L} - \vec{J}_{2R,L} &= i \vec{\xi}_{R,L} \xi_{R,L}^6, \end{aligned} \quad (18)$$

where the triplet of Majorana fermions $\vec{\xi} = (\xi^1, \xi^2, \xi^3)$ accounts for the spin degrees of freedom since the $SU(2)_s$ spin rotation symmetry of the lattice model (1) is generated in the continuum by $\vec{J}_{1R} + \vec{J}_{2R} + R \rightarrow L$. The Majorana fermion ξ^6 is related to the discrete Z_2 interchain exchange as it can be seen from Eq. (18). Finally, the four remaining Majorana fermions can be cast into two pairs, each of which is associated to the two $U(1)$ symmetries in H : $\xi^{4,5}$ (respectively, $\xi^{7,8}$) Majorana fermions describe the orbital (respectively, charge) $U(1)$ symmetry.

With this identification at hand, we can derive the low-energy effective theory for the generalized Hund model (1) at half filling. Assuming only four-fermion (marginal) interactions, the most general model with $H = U(1)_c \times SU(2)_s \times U(1)_o \times Z_2$ invariance can be easily deduced from the Majorana fermion formalism,

$$\begin{aligned} \mathcal{H} = & -\frac{iv_c}{2} \sum_{a=7}^8 (\xi_R^a \partial_x \xi_R^a - \xi_L^a \partial_x \xi_L^a) - \frac{iv_s}{2} \sum_{a=1}^3 (\xi_R^a \partial_x \xi_R^a - \xi_L^a \partial_x \xi_L^a) \\ & - \frac{iv_t}{2} \sum_{a=4}^5 (\xi_R^a \partial_x \xi_R^a - \xi_L^a \partial_x \xi_L^a) - \frac{iv_0}{2} (\xi_R^6 \partial_x \xi_R^6 - \xi_L^6 \partial_x \xi_L^6) \\ & + \frac{g_1}{2} \left(\sum_{a=1}^3 \xi_R^a \xi_L^a \right)^2 + g_2 \left(\sum_{a=1}^3 \xi_R^a \xi_L^a \right) \left(\sum_{a=4}^5 \xi_R^a \xi_L^a \right) \\ & + \xi_R^6 \xi_L^6 \left[g_3 \sum_{a=1}^3 \xi_R^a \xi_L^a + g_4 \sum_{a=4}^5 \xi_R^a \xi_L^a \right] + \frac{g_5}{2} \left(\sum_{a=4}^5 \xi_R^a \xi_L^a \right)^2 \\ & + \frac{g_6}{2} \left(\sum_{a=7}^8 \xi_R^a \xi_L^a \right)^2 + (\xi_R^7 \xi_L^7 + \xi_R^8 \xi_L^8) \\ & \times \left[g_7 \sum_{a=1}^3 \xi_R^a \xi_L^a + g_8 \sum_{a=4}^5 \xi_R^a \xi_L^a + g_9 \xi_R^6 \xi_L^6 \right], \end{aligned} \quad (19)$$

where the normal ordering procedure is assumed here and also in the rest of the paper.

The different velocities and the nine coupling constants cannot be determined within this phenomenological approach based on symmetries. In this respect, a direct standard

continuum limit procedure of the lattice model must be applied. This is done in Appendix A and we find the expression of the velocities

$$\begin{aligned} v_c &= v_F + \frac{a_0}{\pi} \left(\frac{3}{2} U - \frac{J_t}{4} \right), \\ v_s &= v_F - \frac{a_0}{2\pi} \left(U - \frac{J_H}{2} + \frac{J_t}{2} \right), \\ v_t &= v_F - \frac{a_0}{2\pi} \left(U - \frac{3J_t}{2} \right), \\ v_0 &= v_F - \frac{a_0}{2\pi} \left(U + \frac{3J_H}{2} + \frac{J_t}{2} \right) \end{aligned} \quad (20)$$

whereas the identification of the nine coupling constants reads as follows:

$$\begin{aligned} g_1 &= -a_0 \left(U - \frac{J_H}{2} + \frac{J_t}{2} \right), \\ g_2 &= -a_0 \left(U - \frac{J_H}{4} - \frac{J_t}{2} \right), \\ g_3 &= -a_0 \left(U + \frac{J_H}{2} + \frac{J_t}{2} \right), \\ g_4 &= -a_0 \left(U + \frac{3J_H}{4} - \frac{J_t}{2} \right), \\ g_5 &= -a_0 \left(U - \frac{3J_t}{2} \right), \\ g_6 &= a_0 \left(3U - \frac{J_t}{2} \right), \\ g_7 &= a_0 \left(U + \frac{J_H}{4} - \frac{J_t}{2} \right), \\ g_8 &= a_0 \left(U + \frac{J_t}{2} \right), \\ g_9 &= a_0 \left(U - \frac{3J_H}{4} - \frac{J_t}{2} \right). \end{aligned} \quad (21)$$

The main advantage of this Majorana fermions description is that the symmetries of the original lattice model are explicit in the low-energy effective model (19) in sharp contrast to the standard Abelian bosonization representation [see, for instance, Eqs. (A5) and (A7) of Appendix A where the symmetries are hidden]. In particular, using Eqs. (20) and (21), one can check that all extended symmetries of Table I are indeed symmetries of model (19).

B. Duality approach

On top of the continuous symmetries of model (1), the low-energy effective Hamiltonian (19) displays exact hidden discrete symmetries which take the form of duality symmetries. Indeed, as shown recently in Ref. 31, general weakly interacting fermionic models with marginal interactions exhibit nonperturbative duality symmetries in their low-energy description. Those will help us to list and identify possible gapful phases that may occur at low-energy. This is the object of the present section.

The duality symmetries are easily identified here within the Majorana formalism [Eq. (19)] since they are built from Kramers-Wannier duality symmetries^{3,70} of the underlying two-dimensional Ising models associated to the eight Majorana fermions $\xi_{R,L}^a$: they simply take the following form $\xi_L^a \rightarrow -\xi_L^a$, $\xi_R^a \rightarrow \xi_R^a$. Applying the approach of Ref. 31 yields eight possible dualities, that can be built out of three elementary ones that one may choose as

$$\begin{aligned}\Omega_1: \xi_L^{7,8} &\rightarrow -\xi_L^{7,8}, \\ \Omega_2: \xi_L^{4,5} &\rightarrow -\xi_L^{4,5}, \\ \Omega_7: \xi_L^6 &\rightarrow -\xi_L^6.\end{aligned}$$

We now describe in detail each of the eight phases.

1. Spin-Peierls phase

The essence of a duality approach is to relate different phases between themselves. In this respect, we need a starting phase from which the dual phases can be obtained. Such a phase can be most simply chosen by considering the special fine tuning $\Omega_0: g_i = g$ ($i=1, \dots, 9$) in Eq. (19). The RG study presented shortly will assess that this line is attractive under the RG flow. On this particular line of the nine-dimensional parameter space, the interacting part of the low-energy effective model (19) takes the form of the SO(8) Gross-Neveu (GN) model,⁷¹

$$\mathcal{H}_{\text{int}}^{\Omega_0} = \frac{g}{2} \left(\sum_{a=1}^8 \xi_R^a \xi_L^a \right)^2. \quad (22)$$

The SO(8) symmetry rotates the eight Majorana fermions and is the maximal continuous symmetry of the interaction model (19). The SO(8) GN model is integrable and a spectral gap is generated for $g > 0$.^{70,72,73} The resulting phase corresponds to a spin-Peierls (SP) ordering with the lattice order parameter $\mathcal{O}_{\text{SP}} = \sum_{i,l\sigma} (-1)^i c_{l\sigma,i}^\dagger c_{l\sigma,i+1}$.

Indeed, a straightforward semiclassical approach to model (22) reveals that the bosonic fields $\Phi_{c,s,f,sf}$ of the basis [Eq. (A3)] are pinned into the following configurations for $g > 0$:

$$\langle \Phi_a \rangle = \sqrt{\pi} p_a, \quad \langle \Phi_a \rangle = \frac{\sqrt{\pi}}{2} + \sqrt{\pi} q_a, \quad (23)$$

p_a, q_a ($a=c, s, f, sf$) being integers. In addition, the ground-state degeneracy of this phase can be deduced within this semiclassical approach since there is a gauge redundancy in the bosonization procedure (A1),

$$\Phi_{l\sigma R,L} \rightarrow \Phi_{l\sigma R,L} + \sqrt{\pi} p_{l\sigma R,L}, \quad (24)$$

where $p_{l\sigma R,L}$ are integers ($l=1, 2$ and $\sigma = \uparrow, \downarrow$). This transformation leaves intact the Dirac fermion fields $R_{l\sigma}, L_{l\sigma}$. Using the change in basis (A3), we deduce that among the field configurations [Eq. (23)], only two of them are independent [they cannot be connected by the gauge redundancy transformation (24)],

$$\langle \Phi_{c,s,f,sf} \rangle = 0,$$

$$\langle \Phi_c \rangle = \sqrt{\pi}, \quad \langle \Phi_{s,f,sf} \rangle = 0. \quad (25)$$

These two ground states are related by the one-step translation symmetry T_{a_0} , which is described in the bosonization approach by: $\Phi_c \rightarrow \Phi_c + \sqrt{\pi}$. The SP phase is thus twofold degenerate and spontaneously breaks the translation symmetry T_{a_0} as it should.

The continuum bosonized description of the SP order parameter is given by

$$\mathcal{O}_{\text{SP}} \sim \prod_{a=c,s,f,sf} \cos(\sqrt{\pi} \Phi_a) + \prod_{a=c,s,f,sf} \sin(\sqrt{\pi} \Phi_a), \quad (26)$$

from which we deduce that indeed this order parameter condenses in the field configurations [Eq. (25)]: $\langle \mathcal{O}_{\text{SP}} \rangle \neq 0$.

2. Charge-density wave phase

Starting from the SP phase, one can infer all possible gapful phases that may appear at low energy. We obtain a second degenerate phase by performing a duality transformation $\Omega_1: \xi_L^{7,8} \rightarrow -\xi_L^{7,8}$ which is a symmetry of model (19) if $g_{7,8,9} \rightarrow -g_{7,8,9}$. The resulting gapful phase, named \mathcal{M}_1 , is governed by the following interacting Hamiltonian, which replaces the SO(8) line [Eq. (22)],

$$\mathcal{H}_{\text{int}}^{\Omega_1} = \frac{g}{2} \left(\sum_{a=1}^6 \xi_R^a \xi_L^a - \xi_R^7 \xi_L^7 - \xi_R^8 \xi_L^8 \right)^2. \quad (27)$$

In bosonic language, the duality Ω_1 only affects the charge degrees of freedom and corresponds to a simple shift of the charge bosonic field: $\Phi_{cL} \rightarrow \Phi_{cL} + \sqrt{\pi}/2$ and $\Phi_{cR} \rightarrow \Phi_{cR}$. We deduce from Eq. (25) that the phase \mathcal{M}_1 is twofold degenerate with the two semiclassical ground states,

$$\langle \Phi_c \rangle = \frac{\sqrt{\pi}}{2}, \quad \langle \Phi_{s,f,sf} \rangle = 0,$$

$$\langle \Phi_c \rangle = \frac{3\sqrt{\pi}}{2}, \quad \langle \Phi_{s,f,sf} \rangle = 0. \quad (28)$$

Hence, the \mathcal{M}_1 phase also breaks the one-step translation symmetry. The semiclassical approach enables us to identify the \mathcal{M}_1 phase as a CDW phase, described by the lattice order parameter $\mathcal{O}_{\text{CDW}} = \sum_{i,l\sigma} (-1)^i c_{l\sigma,i}^\dagger c_{l\sigma,i}$. Indeed, in the bosonization description, the CDW order parameter reads as follows:

$$\begin{aligned} \mathcal{O}_{\text{CDW}} \sim & \cos(\sqrt{\pi}\Phi_c) \prod_{a=s,f,sf} \sin(\sqrt{\pi}\Phi_a) \\ & - \sin(\sqrt{\pi}\Phi_c) \prod_{a=s,f,sf} \cos(\sqrt{\pi}\Phi_a), \end{aligned} \quad (29)$$

and it obviously condenses in the ground-state configuration (28): $\langle \mathcal{O}_{\text{CDW}} \rangle \neq 0$.

3. Orbital density wave phase

We can define a second duality transformation $\Omega_2: \xi_L^{4,5} \rightarrow -\xi_L^{4,5}$, which is indeed a symmetry of model (19) if $g_{2,4,8} \rightarrow -g_{2,4,8}$. In that case, the SO(8) line [Eq. (22)] is replaced by

$$\mathcal{H}_{\text{int}}^{\Omega_2} = \frac{g}{2} \left(\sum_{a=1,2,3;6,7,8} \xi_R^a \xi_L^a - \xi_R^4 \xi_L^4 - \xi_R^5 \xi_L^5 \right)^2. \quad (30)$$

The duality Ω_2 affects the orbital degrees of freedom and is represented by a shift in the orbital bosonic field: $\Phi_{fL} \rightarrow \Phi_{fL} + \sqrt{\pi}/2$. The resulting phase, \mathcal{M}_2 , is a twofold degenerate with ground-state configurations,

$$\begin{aligned} \langle \Phi_f \rangle &= \frac{\sqrt{\pi}}{2}, \quad \langle \Phi_{c,s,sf} \rangle = 0, \\ \langle \Phi_c \rangle &= \sqrt{\pi}, \quad \langle \Phi_f \rangle = \frac{\sqrt{\pi}}{2}, \quad \langle \Phi_{s,sf} \rangle = 0. \end{aligned} \quad (31)$$

Similarly to the CDW phase, one deduces that \mathcal{M}_2 has a long-range ODW ordering. The order parameter is: $\mathcal{O}_{\text{ODW}} = \sum_{i,l\sigma} (-1)^i (-1)^{l+1} c_{l\sigma,i}^\dagger c_{l\sigma,i}$ whose bosonized form reads

$$\begin{aligned} \mathcal{O}_{\text{ODW}} \sim & \cos(\sqrt{\pi}\Phi_f) \prod_{a=c,s,sf} \sin(\sqrt{\pi}\Phi_a) \\ & - \sin(\sqrt{\pi}\Phi_f) \prod_{a=c,s,sf} \cos(\sqrt{\pi}\Phi_a), \end{aligned} \quad (32)$$

and it obviously condenses in the ground-state configurations [Eq. (31)]: $\langle \mathcal{O}_{\text{ODW}} \rangle \neq 0$.

4. Spin-Peierls- π phase

The last twofold degenerate phase, \mathcal{M}_3 , which breaks translation symmetry, is obtained from the SP phase with help of the duality $\Omega_3 = \Omega_1 \Omega_2: \xi_L^{4,5,7,8} \rightarrow -\xi_L^{4,5,7,8}$. It is a symmetry of model (19) if $g_{2,4,7,9} \rightarrow -g_{2,4,7,9}$. The \mathcal{M}_3 phase is governed by the following interacting Hamiltonian:

$$\mathcal{H}_{\text{int}}^{\Omega_3} = \frac{g}{2} \left(\sum_{a=1,2,3;6} \xi_R^a \xi_L^a - \sum_{a=4,5,7,8} \xi_R^a \xi_L^a \right)^2. \quad (33)$$

The order parameter characterizing the \mathcal{M}_3 phase is a Spin-Peierls- π (SP_π) order parameter with an alternating dimerization profile on the two legs: $\mathcal{O}_{\text{SP}_\pi} = \sum_{i,l\sigma} (-1)^i (-1)^{l+1} c_{l\sigma,i}^\dagger c_{l\sigma,i+1}$. Its bosonized form is

$$\begin{aligned} \mathcal{O}_{\text{SP}_\pi} \sim & \prod_{a=c,f} \cos(\sqrt{\pi}\Phi_a) \prod_{a=s,sf} \sin(\sqrt{\pi}\Phi_a) \\ & + \prod_{a=c,f} \sin(\sqrt{\pi}\Phi_a) \prod_{a=s,sf} \cos(\sqrt{\pi}\Phi_a). \end{aligned} \quad (34)$$

The ground-state configurations of the SP_π phase are given by

$$\begin{aligned} \langle \Phi_{c,f} \rangle &= \frac{\sqrt{\pi}}{2}, \quad \langle \Phi_{s,sf} \rangle = 0, \\ \langle \Phi_c \rangle &= \frac{3\sqrt{\pi}}{2}, \quad \langle \Phi_f \rangle = \frac{\sqrt{\pi}}{2}, \quad \langle \Phi_{s,sf} \rangle = 0, \end{aligned} \quad (35)$$

and $\langle \mathcal{O}_{\text{SP}_\pi} \rangle \neq 0$ in these configurations.

5. Haldane charge phase

So far we have considered only duality symmetries which involve an even number of Majorana fermions. A second class of interesting duality symmetries, called outer dualities in Ref. 31, is involved when an odd number of Majorana fermions is considered. These duality symmetries give rise to the second class of Mott-insulating phases, the nondegenerate ones, which do not spontaneously break the translation symmetry. A first nondegenerate gapful phase, named \mathcal{M}_4 , is obtained from the SO(8) line [Eq. (22)] by the duality $\Omega_4: \xi_L^{6,7,8} \rightarrow -\xi_L^{6,7,8}$. Such an outer duality is a symmetry of model (19) when $g_{3,4,7,8} \rightarrow -g_{3,4,7,8}$. The resulting effective model for the \mathcal{M}_4 phase is

$$\mathcal{H}_{\text{int}}^{\Omega_4} = \frac{g}{2} \left(\sum_{a=1}^5 \xi_R^a \xi_L^a - \sum_{a=6}^8 \xi_R^a \xi_L^a \right)^2. \quad (36)$$

A simple semiclassical analysis of this model shows us that the bosonic fields are pinned in the following way:

$$\begin{aligned} \langle \Phi_c \rangle &= \frac{\sqrt{\pi}}{2} + \sqrt{\pi} p_c, \quad \langle \Phi_{s,f} \rangle = \langle \Theta_{sf} \rangle = \sqrt{\pi} p_{s,f,sf}, \\ \langle \Phi_c \rangle &= \frac{3\sqrt{\pi}}{2} + \sqrt{\pi} q_c, \quad \langle \Phi_{s,f} \rangle = \langle \Theta_{sf} \rangle = \frac{\sqrt{\pi}}{2} + \sqrt{\pi} q_{s,f,sf}, \end{aligned} \quad (37)$$

where $p_a, q_a (a=c,s,f,sf)$ are again integers. Using the gauge redundancy [Eq. (24)], we observe that the phase \mathcal{M}_4 is indeed nondegenerate with ground-state configuration,

$$\langle \Phi_c \rangle = \frac{\sqrt{\pi}}{2}, \quad \langle \Phi_{s,f} \rangle = \langle \Theta_{sf} \rangle = 0. \quad (38)$$

Unfortunately, the order parameter of this \mathcal{M}_4 phase cannot be written locally in terms of the original lattice fermions. In this low-energy procedure, it involves order and disorder operators of the underlying two-dimensional Ising models. The situation here is similar to the RS and RT phases of the two-leg spin- $\frac{1}{2}$ ladder.²⁵ These gapful phases are nondegenerate and display a hidden antiferromagnetic ordering and possibly edge states which can be revealed through non-

local string order parameters.^{26,62,63} In this respect, in order to build those operators, it is useful to introduce the following quantities in terms of the occupation numbers $n_{l\sigma,i}$ of the original lattice fermions:

$$\begin{aligned} n_{c,i} &= \frac{1}{2}(n_{1\uparrow,i} + n_{1\downarrow,i} + n_{2\uparrow,i} + n_{2\downarrow,i}), \\ n_{s,i} &= \frac{1}{2}(n_{1\uparrow,i} - n_{1\downarrow,i} + n_{2\uparrow,i} - n_{2\downarrow,i}), \\ n_{f,i} &= \frac{1}{2}(n_{1\uparrow,i} + n_{1\downarrow,i} - n_{2\uparrow,i} - n_{2\downarrow,i}), \\ n_{sf,i} &= \frac{1}{2}(n_{1\uparrow,i} - n_{1\downarrow,i} - n_{2\uparrow,i} + n_{2\downarrow,i}). \end{aligned} \quad (39)$$

We then consider two classes of stringlike order parameters,

$$\begin{aligned} \mathcal{O}_{a,i}^{\text{even}} &= \cos\left(\pi \sum_{k<i} \delta n_{a,k}\right), \\ \mathcal{O}_{a,i}^{\text{odd}} &= \delta n_{a,i} \cos\left(\pi \sum_{k<i} \delta n_{a,k}\right) \end{aligned} \quad (40)$$

with $\delta n_{a,i} = n_{a,i} - \langle n_{a,i} \rangle$ and $a = c, s, f, sf$. The string operators [Eq. (40)] are, respectively, even or odd under the transformation $\delta n_{a,i} \rightarrow -\delta n_{a,i}$. The bosonization description of these string-order parameters is cumbersome due to the nonlocality of the operators in Eq. (40). A naive continuum expression can be derived with help of its symmetry properties like in the two-leg spin ladder^{63,74} or the one-dimensional extended Bose-Hubbard model,⁷⁵

$$\begin{aligned} \mathcal{O}_a^{\text{even}} &\sim \cos(\sqrt{\pi}\Phi_a), \\ \mathcal{O}_a^{\text{odd}} &\sim \sin(\sqrt{\pi}\Phi_a). \end{aligned} \quad (41)$$

We thus deduce that the odd charge string operator displays long-range ordering in the \mathcal{M}_4 phase,

$$\lim_{|i-j|\rightarrow\infty} \langle \mathcal{O}_{c,i}^{\text{odd}} \mathcal{O}_{c,j}^{\text{odd}} \rangle \sim \lim_{|x-y|\rightarrow\infty} \langle \sin[\sqrt{\pi}\Phi_c(x)] \sin[\sqrt{\pi}\Phi_c(y)] \rangle \neq 0. \quad (42)$$

Using the charge pseudospin operator (7), one immediately observes that this lattice charge string-order parameter is equivalent to the long-range ordering [Eq. (13)] obtained within the strong-coupling approach. We thus conclude that the \mathcal{M}_4 phase is a HC phase which is adiabatically connected to the HC of the strong-coupling approach found in the vicinity of the $J_H = -8U/3$ line. This phase displays a hidden ordering, described by Eq. (42), and pseudospin- $\frac{1}{2}$ edge states, as expected for a Haldane phase. Those (holon) edge states carry charge but are singlet states as far as the spin and orbital degrees of freedom are concerned (see Appendix B). This result will help us to detect numerically the HC phase in the DMRG calculations of Sec. IV.

6. Haldane orbital phase

The next phase, \mathcal{M}_5 , is found by applying the duality symmetries $\xi_L^{4,5,6} \rightarrow -\xi_L^{4,5,6}$ with $g_{2,3,8,9} \rightarrow -g_{2,3,8,9}$. The resulting dual interacting Hamiltonian reads

$$\mathcal{H}_{\text{int}}^{\Omega_5} = \frac{g}{2} \left(\sum_{a=1,2,3,7,8} \xi_R^a \xi_L^a - \sum_{a=4}^6 \xi_R^a \xi_L^a \right)^2. \quad (43)$$

Its ground-state configuration is given by

$$\langle \Phi_f \rangle = \frac{\sqrt{\pi}}{2}, \quad \langle \Phi_{c,s} \rangle = \langle \Theta_{sf} \rangle = 0. \quad (44)$$

The physical properties of the \mathcal{M}_5 phase are very similar to the ones for the HC phase. The orbital degrees of freedom are central to the \mathcal{M}_5 phase and play the role of the charge degrees of freedom for the HC charge. In this respect, the \mathcal{M}_5 phase is characterized by the long-range order of the odd orbital string order parameter,

$$\lim_{|i-j|\rightarrow\infty} \langle \mathcal{O}_{f,i}^{\text{odd}} \mathcal{O}_{f,j}^{\text{odd}} \rangle \sim \lim_{|x-y|\rightarrow\infty} \langle \sin[\sqrt{\pi}\Phi_f(x)] \sin[\sqrt{\pi}\Phi_f(y)] \rangle \neq 0. \quad (45)$$

Using the orbital pseudospin operator (4), we find that the orbital string-order parameter (45) is equivalent to the long-range ordering [Eq. (15)] obtained within the strong-coupling approach. We thus conclude that the \mathcal{M}_5 phase is a HO phase which is adiabatically connected to the HO of the strong-coupling approach found in the vicinity of the $SU(2)_o$ symmetric line $J_t = -3J_H/4$. The HO phase is characterized by pseudospin- $\frac{1}{2}$ edge states (see Appendix B) which carry orbital quantum number only. The orbital edge states will be useful to reveal numerically the HO phase by means of the DMRG approach.

7. Rung-triplet phase

A new nondegenerate phase, named \mathcal{M}_6 , is found by applying the duality symmetry $\Omega_6 \xi_L^{1,2,3} \rightarrow -\xi_L^{1,2,3}$ to the SP phase. The effective interacting Hamiltonian which governs the properties of the \mathcal{M}_6 phase is

$$\mathcal{H}_{\text{int}}^{\Omega_6} = \frac{g}{2} \left(\sum_{a=4}^8 \xi_R^a \xi_L^a - \sum_{a=1}^3 \xi_R^a \xi_L^a \right)^2. \quad (46)$$

In the \mathcal{M}_6 phase, the ground-state configuration for the bosonic fields is

$$\langle \Phi_s \rangle = \langle \Theta_{sf} \rangle = \frac{\sqrt{\pi}}{2}, \quad \langle \Phi_{c,f} \rangle = 0, \quad (47)$$

from which we deduce that the following string-order parameter condenses in this phase:

$$\lim_{|i-j|\rightarrow\infty} \langle \mathcal{O}_{s,i}^{\text{odd}} \mathcal{O}_{s,j}^{\text{odd}} \rangle \sim \lim_{|x-y|\rightarrow\infty} \langle \sin[\sqrt{\pi}\Phi_s(x)] \sin[\sqrt{\pi}\Phi_s(y)] \rangle \neq 0. \quad (48)$$

This order parameter is the standard string-order parameter (11) of the RT phase of the two-leg spin ladder with ferromagnetic interchain coupling. The \mathcal{M}_6 phase is thus a RT phase with spin- $\frac{1}{2}$ edge states.⁶⁶

8. Rung-singlet phase

Finally, the last nondegenerate phase, called \mathcal{M}_7 , is obtained from the $SO(8)$ line [Eq. (22)] by the duality symmetry $\Omega_7: \xi_L^6 \rightarrow -\xi_L^6$. Its effective model is

$$\mathcal{H}_{\text{int}}^{\Omega_7} = \frac{g}{2} \left(\sum_{a=1, a \neq 6}^8 \xi_R^a \xi_L^a - \xi_R^6 \xi_L^6 \right)^2. \quad (49)$$

In the semiclassical approach, the ground-state configuration for the bosons is obtained from the SP one [Eq. (25)] by changing the bosonic field Φ_{s_f} into its dual Θ_{s_f} in the pinning configuration,

$$\langle \Phi_{c,s_f} \rangle = \langle \Theta_{s_f} \rangle = 0. \quad (50)$$

In particular, one observes that no odd string-order parameters can condense into the \mathcal{M}_7 phase. The latter phase is the standard RS phase of the two-leg spin ladder with antiferromagnetic interchain coupling that we have identified in Sec. II within the strong-coupling approach. This phase has no edge state when open-boundary conditions are considered.⁶⁶

C. Phase diagram

The duality symmetry approach, discussed in the previous section, predicts the emergence of eight insulating phases for two-leg electronic ladder with the symmetry group $H = U(1)_c \times SU(2)_s \times U(1)_o \times Z_2$. However, this approach cannot determine which phases actually appear in the phase diagram of a particular model like Eq. (1) with H invariance. To answer this question, we need to perform a one-loop RG calculation of model (19) with initial conditions [Eq. (21)] for the generalized Hund model (1).

1. Phases of the generalized Hund model

The one-loop RG flow of the nine coupling constants of model (19) can be derived by standard methods.^{3,4} By neglecting the velocity anisotropy (i.e., $v_c = v_s = v_o = v_l = v$) and performing a suitable redefinition of the coupling constants ($g_a = 2\pi v f_a$, $a=1, \dots, 9$), we find the one-loop RG equations

$$\dot{f}_1 = f_1^2 + 2f_2^2 + f_3^2 + 2f_7^2,$$

$$\dot{f}_2 = 2f_1f_2 + f_2f_5 + f_3f_4 + 2f_7f_8,$$

$$\dot{f}_3 = 2f_1f_3 + 2f_2f_4 + 2f_7f_9,$$

$$\dot{f}_4 = f_4f_5 + 3f_2f_3 + 2f_8f_9,$$

$$\dot{f}_5 = 3f_2^2 + f_4^2 + 2f_8^2,$$

$$\dot{f}_6 = 3f_7^2 + 2f_8^2 + f_9^2,$$

$$\dot{f}_7 = 2f_1f_7 + 2f_2f_8 + f_3f_9 + f_6f_7,$$

$$\dot{f}_8 = 3f_2f_7 + f_3f_8 + f_4f_9 + f_6f_8,$$

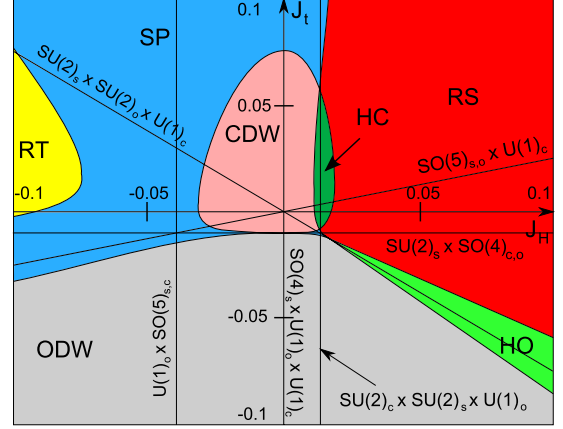


FIG. 2. (Color online) Low-energy phase diagram of the generalized Hund model at half filling for $U = -0.005t$ ($t = 1$). (SP=spin Peierls, CDW=charge-density wave, ODW=orbital density wave, RS=rung singlet, HC=Haldane charge, HO=Haldane orbital, RT=rung triplet). At the intersection of the highly symmetric lines lie points with even larger symmetry (see Table I).

$$\dot{f}_9 = 3f_3f_7 + 2f_4f_8 + f_6f_9. \quad (51)$$

The nine coupling constants of the low-energy Hamiltonian (19) are not independent: they depend only on the three parameters U , J_h , and J_t of the original lattice Hamiltonian (1). We thus need to use the initial conditions [Eq. (21)] to determine which phases do come out in the zero-temperature phase diagram of the generalized Hund model. A numerical analysis of these differential equations, together with the results of the preceding section, gives us the phase diagram of the model. We find seven insulating phases out of the eight possible ones found within the duality approach. The missing phase is the SP_π phase. Of course, by adding next-neighbor interactions to the lattice model (1) without breaking the symmetry group H , the latter phase will be found. Interestingly enough, this lattice model with three independent interactions possess the four nondegenerate Mott-insulating phases that we have revealed with the help the duality symmetry and strong-coupling approaches. In Fig. 2, we present a section of the three-dimensional phase diagram of the generalized Hund model at $U = -0.005$ (t is set to unity) where the seven phases appear.

The duality approach that we used to obtain the phase diagram allows for an easy characterization of the quantum phase transitions. Those transitions are located on the self-dual lines, where the coupling constants that change their sign when going from one phase to the other vanish. Figure 3 summarizes all the phase transitions that occur in the phase diagram of the generalized Hund model.

We now present the zero-temperature phase diagram of several interesting highly symmetric models with two independent coupling constants that we have introduced in Sec. II.

2. Phase diagram of the $SO(5)$ fermionic cold atoms model

Let us start with the spin- $\frac{3}{2}$ cold fermionic atoms model (6) which is obtained from the generalized Hund model (1)

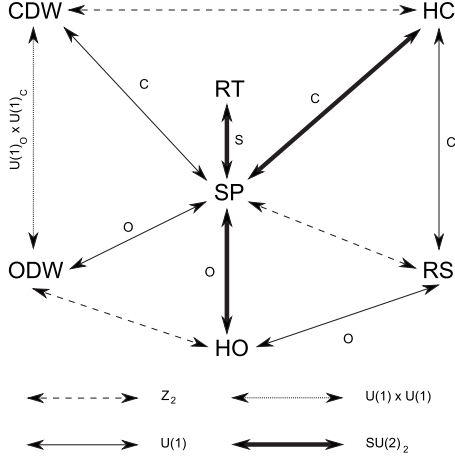


FIG. 3. Quantum phase transitions that can occur in the generalized Hund model. The letter next to the arrows indicates which degrees of freedom are critical: c =charge, s =spin, and o =orbital.

by the fine tuning $J_H=4J_t$. In the continuum limit, the coupling constants are naturally parametrized by the singlet and quintet pairing U_0 and U_2 : $g_1=g_2=g_5=-U_0-U_2$, $g_3=g_4=U_0-3U_2$, $g_6=U_0+5U_2$, $g_7=g_8=2U_2$, $g_9=2U_0$. The effective Majorana model (19), describing the physical properties of the spin- $\frac{3}{2}$ cold fermions model, depends on five independent coupling constants. The resulting phase diagram, as obtained from the one-loop RG calculation, is presented in Fig. 4.

3. $SO(5)$ SZH model

As mentioned in Sec. I, there is a second $SO(5)$ -symmetric model embedded in the generalized Hund model (1): the SZH model (8). In the latter model, obtained from Eq. (1) when $J_H=8U$, the $SO(5)$ symmetry unifies charge and spin degrees of freedom.⁶ The coupling constants of the Majorana model (19) for the SZH model (8) read as follows:

$$\begin{aligned} g_{1,6,7} &= a_0(U_{\text{SZH}} + 2V_{\text{SZH}}), \\ g_{2,8} &= a_0U_{\text{SZH}}, \\ g_{3,9} &= -a_0(3U_{\text{SZH}} + 2V_{\text{SZH}}), \\ g_4 &= -a_0(3U_{\text{SZH}} + 4V_{\text{SZH}}), \\ g_5 &= a_0(U_{\text{SZH}} - 2V_{\text{SZH}}). \end{aligned} \quad (52)$$

We obtain the phase diagram shown in Fig. 5. The phases are very similar to the one in the spin- $\frac{3}{2}$ cold fermions model with the substitution: $CDW \rightarrow ODW$ and $HC \rightarrow HO$.

4. Phase diagram of $SO(4)$ models

We now turn to models which display an extended $SO(4)$ symmetry. In Sec. II, we found two different $SO(4)$ models with two independent coupling constants, i.e., one fine tuning with respect to the original generalized Hund model (1). When $J_H=0$, the lattice model (5) enjoys a $U(1)_c \times U(1)_o$

$\times SO(4)_s$ continuous symmetry. The phase diagram of this model can be determined by the low-energy approach from the identification of the coupling constants of model (19),

$$g_1 = g_3 = -a_0 \left(U + \frac{J_t}{2} \right),$$

$$g_2 = g_4 = -a_0 \left(U - \frac{J_t}{2} \right),$$

$$g_5 = -a_0 \left(U - \frac{3J_t}{2} \right),$$

$$g_6 = a_0 \left(3U - \frac{J_t}{2} \right),$$

$$g_7 = g_9 = -g_2 = -g_4,$$

$$g_8 = -g_1 = -g_3. \quad (53)$$

The resulting phase diagram is presented in Fig. 6. It contains an interesting line $J_t=2U$ with enlarged $SO(4)_{c,o} \times SO(4)_s$ symmetry (see Sec. II). It is straightforward to see that along this line for $U < 0$, where the transition between the CDW and ODW appears, the spin degrees of freedom are gapped while the charge and orbital degrees of freedom are critical. Hence, the quantum phase transition is described by a $SO(4)_1$ CFT with central charge $c=2$.

The second model is defined for $J_t=2U$ (see Table I) with $SO(4)_{c,o} \times SU(2)_s$ continuous symmetry. Here, the $SO(4)$ symmetry unifies the charge and orbital degrees of freedom. The coupling constants of the continuum limit of this model are given by

$$\begin{aligned} g_1 &= -a_0 \left(2U - \frac{J_H}{2} \right), \\ g_2 = g_7 &= a_0 \frac{J_H}{4}, \end{aligned}$$

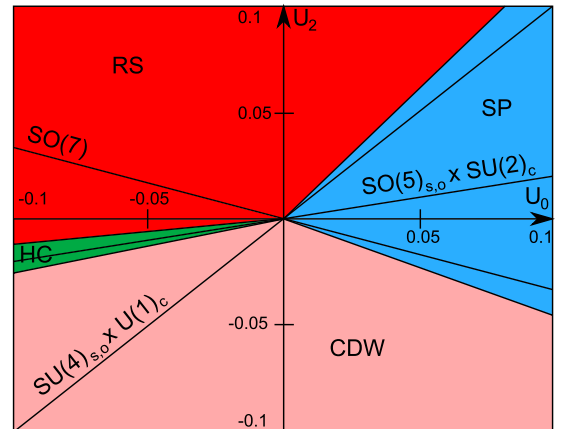


FIG. 4. (Color online) Phase diagram of the spin- $\frac{3}{2}$ cold fermions model at half filling ($t=1$).

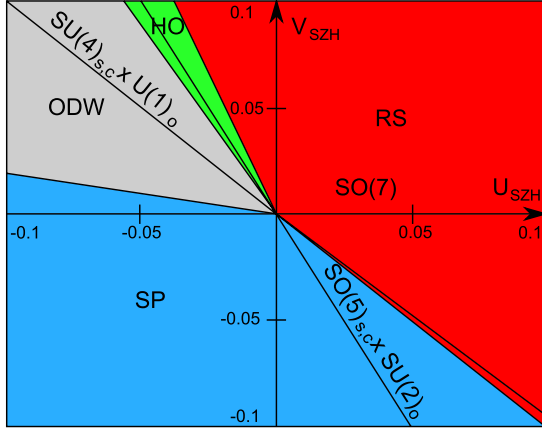


FIG. 5. (Color online) Phase diagram of the SZH model (8) with the fine tuning $J_{SZH}=4(U_{SZH}+V_{SZH})$ at half filling ($t=1$).

$$\begin{aligned}
 g_3 &= -a_0 \left(2U + \frac{J_H}{2} \right), \\
 g_4 = g_9 &= -a_0 \frac{3J_H}{4}, \\
 g_5 = g_6 = g_8 &= 2a_0U,
 \end{aligned} \tag{54}$$

from which we deduce the phase diagram of Fig. 7. The quantum phase transition between RS and RT phases for $J_H=0$ and $U>0$ is now governed by the spin degrees freedom and the $SO(4)_1$ CFT.

5. Phase diagram of spin-orbital (charge) models

The generalized Hund model (1) reduces to the spin-orbital model when $J_i=-3J_H/4$ with a $U(1)_c \times SU(2)_o \times SU(2)_s$ symmetry which has been studied in the context of orbital degeneracy.³⁵⁻³⁹ The coupling constants of the continuum limit of this model read as follows:

$$g_1 = -a_0 \left(U - \frac{7J_H}{8} \right),$$

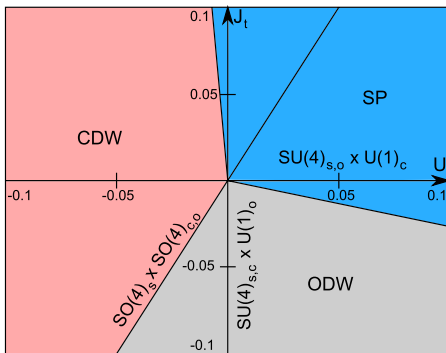


FIG. 6. (Color online) Phase diagram of the $SO(4)$ model (5) with $J_H=0$ ($t=1$) at half filling. The continuous symmetry group is $U(1)_c \times U(1)_o \times SO(4)_s$.

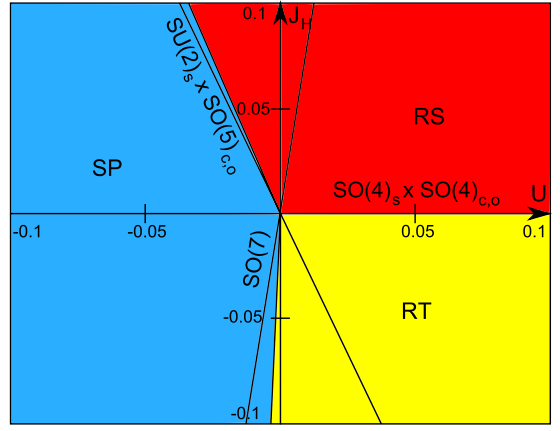


FIG. 7. (Color online) Phase diagram of the half-filled $SO(4)$ model with $J_i=2U$ ($t=1$) which unifies charge and orbital degrees of freedom.

$$\begin{aligned}
 g_2 = g_3 &= -a_0 \left(U + \frac{J_H}{8} \right), \\
 g_4 = g_5 &= -a_0 \left(U + \frac{9J_H}{8} \right), \\
 g_6 &= a_0 \left(3U + \frac{3J_H}{8} \right), \\
 g_7 &= a_0 \left(U + \frac{5J_H}{8} \right), \\
 g_8 = g_9 &= a_0 \left(U - \frac{3J_H}{8} \right).
 \end{aligned} \tag{55}$$

The phase diagram of the spin-orbital model is presented in Fig. 8. In particular, it includes two nondegenerate Mott-insulating phases: HO and RT phases.

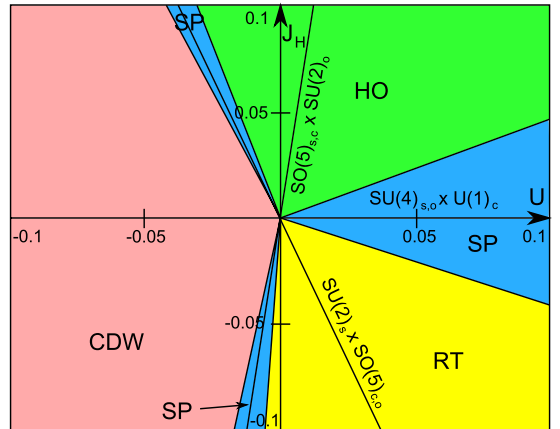


FIG. 8. (Color online) Phase diagram of the spin-orbital model at half filling with $J_i=-3J_H/4$ ($t=1$).

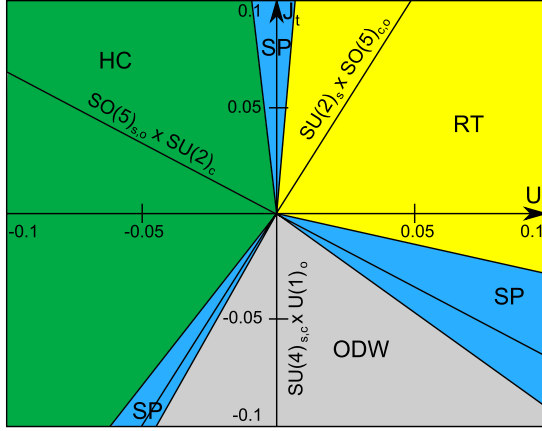


FIG. 9. (Color online) Phase diagram of the spin-charge model at half filling with $J_H = -8U/3$ ($t=1$). The symmetry is $SU(2)_s \times SU(2)_c \times U(1)_o$.

Finally, we consider the related spin-charge model which is defined for the fine tuning $J_H = -8U/3$ with $U(1)_o \times SU(2)_c \times SU(2)_s$ continuous symmetry at half filling. The resulting model is similar to the spin-orbital model where now spin and charge are put on the same footing. We find the following continuum limit for the spin-charge model:

$$\begin{aligned}
 g_1 &= -a_0 \left(\frac{7U}{3} + \frac{J_t}{2} \right), \\
 g_2 &= -a_0 \left(\frac{5U}{3} - \frac{J_t}{2} \right), \\
 g_3 &= g_7 = a_0 \left(\frac{U}{3} - \frac{J_t}{2} \right), \\
 g_4 &= g_8 = a_0 \left(U + \frac{J_t}{2} \right), \\
 g_5 &= -a_0 \left(U - \frac{3J_t}{2} \right), \\
 g_6 &= g_9 = a_0 \left(3U - \frac{J_t}{2} \right). \quad (56)
 \end{aligned}$$

Its phase diagram is depicted in Fig. 9. Here, two nondegenerate Mott insulating phases appear: the HC and RT phases.

D. Effect of an interchain hopping term

Let us now consider the generalized Hund model (1) to which we add an interchain hopping term,

$$\mathcal{H}_\perp = -t_\perp \sum_{i,\sigma} (c_{1\sigma,i}^\dagger c_{2\sigma,i} + \text{H.c.}). \quad (57)$$

This problem has been previously studied and its phases are known.^{5,11,12} We will show that all those phases (there are eight of them) can be connected one-by-one (by a nontrivial

duality) to the phases of the generalized Hund model (1). Our approach will use a weak coupling analysis, and our conclusion relies on the existence of a hidden orbital symmetry emerging at low energy. In Appendix C, we show that this approach is also valid in the strong-coupling regime, close to the orbital line $J_t = -3J_H/4$.

In the presence of interchain hopping, the noninteracting part of the Hamiltonian cannot be readily diagonalized. We need to do a change in basis and introduce bonding and antibonding operators,

$$d_{j\sigma} = \frac{1}{\sqrt{2}} [c_{1\sigma} + (-1)^j c_{2\sigma}]. \quad (58)$$

Using this basis, the kinetic part can be diagonalized in momentum space; there are now two decoupled bands (bonding and antibonding bands) and two Fermi points (provided $t_\perp < 2t$) k_{F1} and k_{F2} such that, at half filling, $k_{F1} + k_{F2} = \pi/a_0$. One could proceed by linearizing around the four Fermi points, by introducing continuous bonding and antibonding fermionic fields $R_{a\sigma}(x)$ and $L_{a\sigma}(x)$ (with $a=1,2$, $\sigma = \uparrow, \downarrow$) by bosonizing, refermionizing, and expanding the interactions in this basis. Instead, we will follow an approach that is based on the (continuous) symmetry content of the theory, by showing that the symmetry of the low energy, continuous theory is essentially the *same* for $t_\perp \neq 0$ as for $t_\perp = 0$.

This is not obvious: naively, the interchain hopping term breaks the $U(1)_o$ orbital symmetry and the analysis of the preceding sections breaks down. However, as noticed before,^{5,12} at low energy another $U(1)$ symmetry emerges in the orbital sector. To see this, let us consider the difference $\delta = k_{F1} - k_{F2} = 2 \arcsin(t_\perp/2t)$. It is a continuous function of t_\perp , and provided δ is not commensurate to π , in the continuum limit and at weak coupling, one can safely ignore umklapp terms that oscillate at wave vector that are integer multiples of δ . Retaining only marginal, four-fermion interactions of the form $\prod_{i=1}^4 \Psi_{a,\sigma_i}^{(i)}$, with $\Psi^{(i)} = R, L$, one sees that in order for this term to be nonoscillating and to give a contribution to the interacting part of the continuous theory, it has to conserve *separately* the quantities $\rho_+ = N_{1R} + N_{2L}$ and $\rho_- = N_{1L} + N_{2R}$, where $N_{aL} = \sum_{\sigma} \int dx L_{a\sigma}^\dagger L_{a\sigma}$ and $N_{aR} = \sum_{\sigma} \int dx R_{a\sigma}^\dagger R_{a\sigma}$ are the total number of left (right) fermions in each of the bonding and antibonding bands. It results that the difference $\rho_+ - \rho_- = (N_{1R} - N_{2R}) - (N_{1L} - N_{2L})$ is conserved: this is nothing but (twice) the total orbital current in the bonding/antibonding basis along direction z . This quantity generates a $U(1)$ orbital symmetry $\widetilde{U}(1)_o$. One thus concludes that the low-energy continuous theory has a symmetry $U(1)_c \times SU(2)_s \times \widetilde{U}(1)_o \times Z_2$, the same as in the $t_\perp = 0$ case.

The total orbital current $\rho_+ - \rho_-$ can be mapped onto the total orbital charge [all other conserved quantities, i.e., the electric charge and the $SU(2)_s$ spin generators, being unaffected] by the duality Ω_\perp that leaves all Majorana fermions $(\xi^a)_{a \neq 5}$ invariant but changes ξ_L^5 to $-\xi_L^5$. The duality Ω_\perp is highly nonlocal. A little algebra shows that it has the following action on the bonding and antibonding modes ($a=1,2$):

$$L_{a\uparrow} \mapsto L_{a\downarrow}^\dagger, \quad L_{a\downarrow} \mapsto -L_{a\uparrow}^\dagger. \quad (59)$$

TABLE II. Pattern of the bosonic fields pinning for $t_{\perp}=0$ and $t_{\perp} \neq 0$.

Phase	$\langle \Phi_c \rangle$	$\langle \Phi_s \rangle$	$\langle \Phi_f \rangle$	$\langle \Theta_f \rangle$	$\langle \Phi_{sf} \rangle$	$\langle \Theta_{sf} \rangle$
SP	0	0	0		0	
CDW	$\sqrt{\pi}/2$	0	0		0	
ODW	0	0	$\sqrt{\pi}/2$		0	
SP_{π}	$\sqrt{\pi}/2$	0	$\sqrt{\pi}/2$		0	
RS	0	0	0			0
HC	$\sqrt{\pi}/2$	0	0			0
HO	0	0	$\sqrt{\pi}/2$			0
RT	0	$\sqrt{\pi}/2$	0			$\sqrt{\pi}/2$
S-Mott	0	0		$\sqrt{\pi}/2$	0	
S'-Mott	$\sqrt{\pi}/2$	0		$\sqrt{\pi}/2$	0	
D-Mott	0	0		0	0	
D'-Mott	$\sqrt{\pi}/2$	0		0	0	
CDW_{π}	0	0		$\sqrt{\pi}/2$		0
PDW	$\sqrt{\pi}/2$	0		$\sqrt{\pi}/2$		0
SF	0	0		0		0
FDW	0	$\sqrt{\pi}/2$		$\sqrt{\pi}/2$		$\sqrt{\pi}/2$

With those elements at hand, the general form of the low-energy Hamiltonian can thus be readily deduced from (19) by performing the replacement $\xi_L^5 \rightarrow -\xi_L^5$. While this approach tells nothing about the (bare) value of the coupling constants g_a , it tells us that the structure of the RG Eq. (51) is the same, and is thus sufficient to (i) enumerate the phases of the model and (ii) relate each of those phases to the phases of the generalized Hund model (1).

From the preceding sections ($t_{\perp}=0$), we deduce that there are eight possible insulating phases. The effect of the duality Ω_{\perp} is to transform the bosonic field Φ_f into its dual with a shift of $\sqrt{\pi}/2$: $\Phi_f \rightarrow \Theta_f + \sqrt{\pi}/2$. We then obtain the pinnings of the bosonic fields from those found for $t_{\perp}=0$ via the duality Ω_{\perp} ; they are summarized in Table II. In the language of Ref. 31, Ω_{\perp} is an outer duality (it affects only one Majorana fermion, or equivalently, it maps a bosonic field onto its dual): it results that it maps degenerate phases onto nondegenerate ones and vice versa.

The pinnings of Table II allow us to identify each phase with one of the already known phases of the generalized two-leg Hubbard ladder.^{5,11,12} The SP phase becomes an S-Mott phase with order parameter,

$$\mathcal{O}_{\text{S-Mott}} = \sum_{i,l} c_{l\uparrow,i} c_{l\downarrow,i}. \quad (60)$$

The CDW phase becomes the D-Mott phase, which is the same phase as RS, and is characterized by the order parameter,

$$\mathcal{O}_{\text{D-Mott}} = \sum_i c_{1\uparrow,i} c_{2\downarrow,i} - c_{2\uparrow,i} c_{1\downarrow,i}. \quad (61)$$

The ODW (respectively, SP_{π}) phase give an S'-Mott (respectively, D'-Mott) state which differs from the S-Mott (respectively, D-Mott) only in the pinning of the charge bosonic field Φ_c (see Table II).¹¹ Such order parameters have the

slowest decaying correlation function when the system is doped. The nondegenerate RS phase will become the twofold degenerate CDW_{π} phase with an interleg phase difference,⁷⁶

$$\mathcal{O}_{\text{CDW-}\pi} = \sum_{i,l\sigma} (-1)^i (-1)^{l+1} c_{l\sigma,i}^{\dagger} c_{l\sigma,i}. \quad (62)$$

The HC phase becomes a p-density wave (PDW) phase which is described by the condensation of the order parameter,⁷⁷

$$\mathcal{O}_{\text{PDW}} = \sum_{i,l\sigma} (-1)^i (-1)^{l+1} (c_{l\sigma,i}^{\dagger} c_{l\sigma,i+1} + \text{H.c.}). \quad (63)$$

The HO phase gives a staggered flux (SF) phase (or a DDW phase) whose ground states display currents circulating around a plaquette, with order parameter

$$\mathcal{O}_{\text{SF}} = i \sum_{i,\sigma} (c_{1\sigma,i}^{\dagger} c_{2\sigma,i} + c_{2\sigma,i}^{\dagger} c_{2\sigma,i+1} + c_{2\sigma,i+1}^{\dagger} c_{1\sigma,i+1} + c_{1\sigma,i+1}^{\dagger} c_{1\sigma,i} - \text{H.c.}). \quad (64)$$

This phase spontaneously breaks time-reversal symmetry. Finally, the RT phase will become a f-density wave (FDW). This phase consists in currents flowing along the diagonals of plaquettes:

$$\mathcal{O}_{\text{FDW}} = i \sum_{i,\sigma} (c_{2\sigma,i+1}^{\dagger} c_{1\sigma,i} - c_{1\sigma,i}^{\dagger} c_{2\sigma,i+1} + c_{1\sigma,i+1}^{\dagger} c_{2\sigma,i} - c_{2\sigma,i}^{\dagger} c_{1\sigma,i+1}). \quad (65)$$

It also breaks time-reversal symmetry.

As already emphasized, the emergent duality symmetry Ω_{\perp} provides only a correspondence between the set of phases with $t_{\perp}=0$ with those of $t_{\perp} \neq 0$. By no means, it maps a given model defined by $(t_{\perp}=0, U, J_H, J_t)$ onto the model $(t_{\perp} \neq 0, U, J_H, J_t)$. In this respect, it is necessary to use the one-loop RG calculation to map out the phase diagram of the

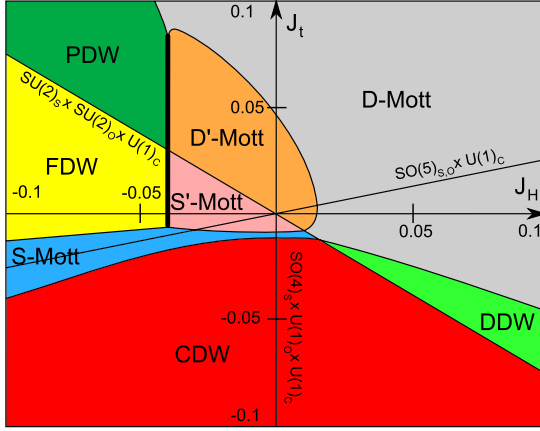


FIG. 10. (Color online) The eight fully gapped phases of the generalized Hund chain with a transverse hopping at half filling ($U = -0.005t$).

generalized Hund chain with a transverse hopping. Using Eq. (51) and the initial conditions for that model,

$$\begin{aligned}
 g_1 &= a_0 \left(-U + \frac{J_H}{2} - \frac{J_t}{2} \right), \\
 g_2 &= a_0 \left(-\frac{3J_H}{8} - \frac{J_t}{2} \right), \\
 g_3 &= a_0 \left(-U + \frac{J_H}{4} + \frac{J_t}{2} \right), \\
 g_4 &= g_2, \\
 g_5 &= a_0 \left(U + \frac{3J_H}{4} - \frac{J_t}{2} \right), \\
 g_6 &= a_0 \left(3U - \frac{J_t}{2} \right), \\
 g_7 &= a_0 \left(U + \frac{J_H}{4} - \frac{J_t}{2} \right), \\
 g_8 &= g_2, \\
 g_9 &= a_0 \left(U + \frac{J_t}{2} \right), \tag{66}
 \end{aligned}$$

we find the presence of the eight insulating phases. Figure 10 presents a section of the phase diagram for $U = -0.005t$ where the eight phases are revealed. Interestingly enough, the generalized Hund chain model with a transverse hopping turns out to be the minimal model for two-leg electronic ladder models which contains the eight insulating phases found within the low-energy approach.^{11,12} In particular, one does not need to add further interactions (first neighbors density interactions, for instance) contrarily to Refs. 11 and 12.

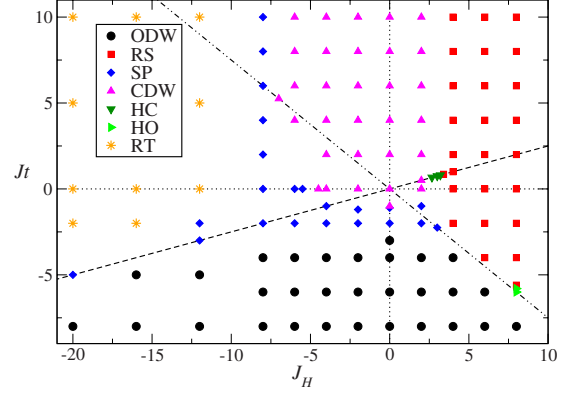


FIG. 11. (Color online) Numerical phase diagram of the generalized Hund model at half filling for $U = -t$. Notations are the same as in Fig. 2.

IV. DMRG CALCULATIONS

We now carry out numerical calculations using DMRG in order to investigate the various phase diagrams. For simplicity, we will restrict ourselves to the $t_{\perp} = 0$ case for which we can use a purely one-dimensional implementation of the model. Moreover, for a system of finite size L , we can fix the total number of particles $N = 2Q_c = 2\sum_i n_{c,i} = 2L$, the z component of the total spin $S^z = \sum_i n_{s,i}$ as well as the z component of the total orbital operator $T^z = \sum_i n_{f,i}$ [see Eq. (39)] so that the states are labeled by the triplet (Q_c, S^z, T^z) . Typically, we keep up to 1600 states, which allow to have an error below 10^{-6} , and we use OBCs.

As it has been revealed by the low-energy approach, there are eight possible insulating phases, which are related by duality transformations. In order to characterize them, we can either compute local quantities (bond kinetic energy, local density, etc.) to identify states that break a given symmetry, or investigate the presence or absence of various edge states to detect nondegenerate Mott phases. Thus, the three possible Haldane phases that have been predicted (RT, HC, and HO) can be characterized by looking for the presence of edge states with quantum numbers (Q_c, S_z, T_z) , respectively, equal to $(L, 1, 0)$, $(L+1, 0, 0)$, and $(L, 0, 1)$ (see details in Appendix B).

From these measurements, we can draw various cuts of the phase diagram in the (U, J_H, J_t) parameter space. In Fig. 11, we present our data for fixed $U = -t$. Seven (out of eight) insulating phases are found and the overall topology nicely agrees with the low-energy predictions shown in Fig. 2, although those were obtained with a much weaker interaction $U = -0.005t$. As another example, we consider a highly symmetric case, namely, the SZH model (see Sec. III C 3), which corresponds to the case $J_H = 8U$. We recall that the low-energy phase diagram of this model is shown in Fig. 5. The numerical phase diagram (Fig. 12) is in excellent agreement not only for the overall topology but also for the location of the phase boundaries.

Finally, we also did simulations for the spin-orbital model obtained by fixing $J_t = -3J_H/4$. In that case as well, we observe that the low-energy predictions (see Fig. 8) and our numerical data (see Fig. 13) coincide very well.

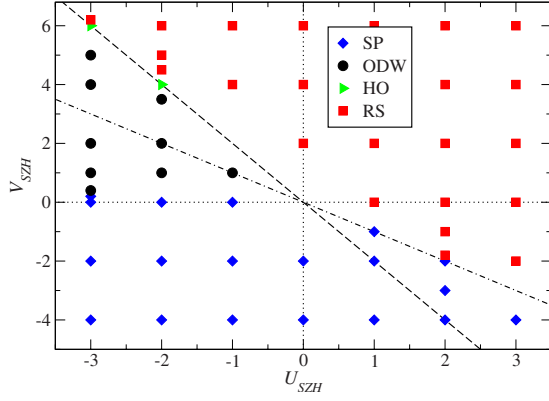


FIG. 12. (Color online) Numerical phase diagram of the SZH SO(5) model with the fine tuning $J_{\text{SZH}}=4(U_{\text{SZH}}+V_{\text{SZH}})$ at half filling. Notations are the same as in Fig. 5. Dashed lines indicate models with higher symmetry (see Table I).

In brief, for all the cases we considered when $t_{\perp}=0$, we obtain an excellent agreement between the low-energy predictions (obtained for very weak couplings) and the numerical phase diagram (obtained at moderate couplings). This is an important result of our paper.

The case of a transverse hopping $t_{\perp} \neq 0$ is much more difficult to analyze with respect to the low-energy approach. As discussed in Sec. III D, in the latter approach, there is an emergent $U(1)$ symmetry in the orbital space which is not present on the lattice. It means that we need to consider long-size systems in the DMRG calculations in order to compare with the low-energy predictions. A second difficulty arises with respect to the numerical discrimination between the S-Mott (respectively, D-Mott) phase and the S'-Mott (respectively, D'-Mott) phase. A numerical analysis of relevant string-order parameters is clearly called for to distinguish them. To the best of our knowledge, we are not aware of any numerical study which reports the existence of the (S,D)-Mott phases in generalized two-leg electronic ladders. We plan to investigate elsewhere the numerical phase diagram of the generalized Hund model with a transverse hopping.

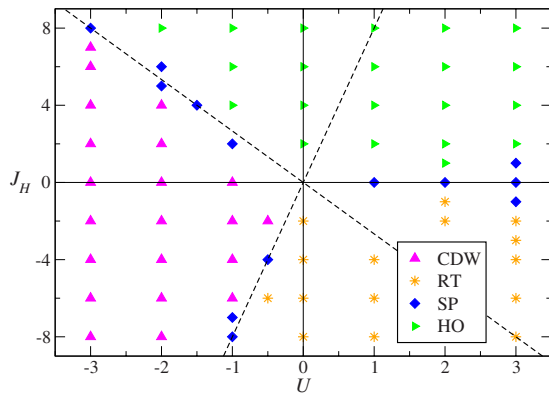


FIG. 13. (Color online) Numerical phase diagram of the spin-orbital model ($J_t=-3J_H/4$) at half filling. Notations are the same as in Fig. 8. Dashed lines indicate models with higher symmetry (see Table I).

V. CONCLUDING REMARKS

In summary, we have investigated the phase diagram of the generalized Hund model (1) with global symmetry group $H=U(1)_c \times SU(2)_s \times U(1)_o \times Z_2$ at half filling by means of complementary low-energy and DMRG techniques. The interest of this model is manifold. First, it covers and unifies several highly symmetric lattice models: the SO(5)-symmetric model describing spin- $\frac{3}{2}$ cold fermions; another (different) SO(5)-symmetric model introduced by Scalapino, Zhang, and Hanke that unifies antiferromagnetism and d -wave superconductivity; and two $SU(2) \times SU(2)$ -symmetric spin-orbital models. While its orbital $U(1)$ symmetry can seem a little odd from the point of view of applications to the description of Hubbard two-leg ladders, we show that at weak coupling, it shares the same continuous low-energy effective theory with the well known Hubbard two-leg ladder with interchain hopping. Third, it is directly relevant to the description of ytterbium 171 loaded into an optical 1D trap. We are able to treat on an equal footing all the phases appearing in those models coming from different contexts. The rich phase diagram of the generalized Hund model has to be contrasted with the minimal character and simplicity of this model, which only depends on three microscopic couplings.

We briefly recall our main results: by means of a duality approach, we predict that the phase diagram for half-filled four-component fermions with global symmetry $H=U(1)_c \times SU(2)_s \times U(1)_o \times Z_2$ consists in eight Mott-insulating phases. These phases fall into two different classes. A first class consists of twofold degenerate fully gapped density phases which spontaneously break a discrete symmetry present on the lattice. The second class comprises four non-degenerate Mott-insulating phases which are characterized by nonlocal string order parameters: RS, RT, HC, and HO phases. A one-loop RG calculation for model (1) reveals the existence of seven phases out of the eight ones consistent with the duality approach. The missing phase, which can be found by adding further nearest-neighbor interactions, is an alternating bond ordered phase (SP_{π}). These results have been confirmed numerically by means of a DMRG approach for moderate couplings. In this respect, we found an excellent agreement between the two complementary approaches.

Finally, we have connected our low-energy results to the eight previously known insulating phases found in generalized two-leg ladders with a transverse hopping t_{\perp} term. When $t_{\perp} \neq 0$, the $U(1)$ orbital symmetry is lost on the lattice but becomes an emergent symmetry at low energy. The duality approach with global symmetry group H can then still be applied in the presence of an interchain hopping t_{\perp} term. In this respect, we discovered a nonlocal duality which maps the eight Mott-insulating phases for $t_{\perp}=0$ onto the eight phases previously known for $t_{\perp} \neq 0$. The one-loop RG approach to the generalized Hund model with interchain hopping predicts the stabilization of the eight Mott-insulating phases. The latter model is thus the minimal model for two-leg electronic ladders which displays the eight Mott-insulating phases at weak coupling. We also discuss the fate of this emergent $U(1)$ orbital symmetry when going from the weak-coupling to the strong-coupling regime. We show that

the weak- and strong-coupling phases coincide in the vicinity of the orbital symmetric line but our analysis suggests a breakdown of this picture away from this special line.

We hope that future experiments on ^{171}Yb or alkaline-earth cold fermions atoms loaded into a 1D optical lattice will reveal some of the exotic insulating phases found in our study.

ACKNOWLEDGMENTS

We would like to thank P. Azaria and G. Roux for collaborations on related problems. P.L. is very grateful to the department of physics, university of Gothenburg for hospitality during the completion of this work. S.C. thanks CALMIP for allocation of CPU time.

APPENDIX A: CONTINUUM LIMIT

In this appendix, we present the technical details of the continuum limit of the generalized Hund model (1). The starting point of the low-energy approach is the linearization around the Fermi points $\pm k_F$ of the dispersion relation for noninteracting fermions. Four left- and right-moving Dirac fermions $L_{l\sigma}, R_{l\sigma}$ ($l=1, 2$ and $\sigma=\uparrow, \downarrow$) are then introduced to describe the lattice fermions $c_{l\sigma,i}$ in the continuum limit [see Eq. (16)].

The next step of the approach is the introduction of four chiral bosonic fields $\Phi_{l\sigma R, L}$ through the Abelian bosonization of Dirac fermions,^{3,4}

$$\begin{aligned} R_{l\sigma} &= \frac{\kappa_{l\sigma}}{\sqrt{2\pi a_0}} \exp(i\sqrt{4\pi}\Phi_{l\sigma R}), \\ L_{l\sigma} &= \frac{\kappa_{l\sigma}}{\sqrt{2\pi a_0}} \exp(-i\sqrt{4\pi}\Phi_{l\sigma L}), \end{aligned} \quad (\text{A1})$$

where the bosonic fields satisfy the following commutation relation:

$$[\Phi_{l\sigma R}, \Phi_{l'\sigma' L}] = \frac{i}{4} \delta_{ll'} \delta_{\sigma\sigma'}. \quad (\text{A2})$$

The presence of the Klein factors $\kappa_{l\sigma}$ ensures the correct anticommutation of the fermionic operators. The Klein factors satisfy the anticommutation rule $\{\kappa_{l\sigma}, \kappa_{l'\sigma'}\} = 2\delta_{ll'} \delta_{\sigma\sigma'}$ and they are constrained so that $\Gamma^2=1$, with $\Gamma = \kappa_{1\uparrow}\kappa_{1\downarrow}\kappa_{2\uparrow}\kappa_{2\downarrow}$. Hereafter, we will work within the $\Gamma=1$ sector. It will be convenient to work with a pair of dual non-chiral bosonic fields: $\Phi_{l\sigma} = \Phi_{l\sigma L} + \Phi_{l\sigma R}$ and $\Theta_{l\sigma} = \Phi_{l\sigma L} - \Phi_{l\sigma R}$. Last, let us introduce a $\text{SU}(4)$ basis that will allow us to separate charge and non-Abelian (spin) degrees of freedom,

$$\begin{aligned} \Phi_{1\uparrow} &= \frac{1}{2}(\Phi_c + \Phi_s + \Phi_f + \Phi_{sf}), \\ \Phi_{1\downarrow} &= \frac{1}{2}(\Phi_c - \Phi_s + \Phi_f - \Phi_{sf}), \\ \Phi_{2\uparrow} &= \frac{1}{2}(\Phi_c + \Phi_s - \Phi_f - \Phi_{sf}), \end{aligned}$$

$$\Phi_{2\downarrow} = \frac{1}{2}(\Phi_c - \Phi_s - \Phi_f + \Phi_{sf}). \quad (\text{A3})$$

In sharp contrast with incommensurate fillings, there is no spin charge separation at half filling. Indeed, in this special case, chiral umklapp processes couple those degrees of freedom. Consequently, the resulting low-energy Hamiltonian corresponding to model (1) takes the form: $\mathcal{H} = \mathcal{H}_c + \mathcal{H}_s + \mathcal{H}_{\text{umklapp}}$.

The charge degrees of freedom are described by

$$\mathcal{H}_c = \frac{v_F}{2} [(\partial_x \Phi_c)^2 + (\partial_x \Theta_c)^2] + \Delta v_c (\partial_x \Phi_c)^2, \quad (\text{A4})$$

where $v_F = a_0 t$ is the Fermi velocity.

The part of the bosonized Hamiltonian corresponding to the nonabelian degrees of freedom is

$$\begin{aligned} \mathcal{H}_s &= \frac{v_F}{2} \sum_{a=s,f,sf} [(\partial_x \Phi_a)^2 + (\partial_x \Theta_a)^2] + \sum_{a=s,f,sf} \Delta v_a (\partial_x \Phi_a)^2 \\ &+ A_1 (C_{sfR}^{\sqrt{16\pi}} + C_{sfL}^{\sqrt{16\pi}}) + A_2 (C_s^{\sqrt{4\pi}} + C_f^{\sqrt{4\pi}}) \tilde{C}_{sf}^{\sqrt{4\pi}} \\ &+ A_3 C_s^{\sqrt{4\pi}} C_f^{\sqrt{4\pi}} + A_4 C_s^{\sqrt{4\pi}} C_{sf}^{\sqrt{4\pi}} + A_5 C_f^{\sqrt{4\pi}} C_{sf}^{\sqrt{4\pi}}, \end{aligned} \quad (\text{A5})$$

where we used the compact notation: $C_a^\beta = \cos(\beta\Phi_a)$, and $\tilde{C}_a^\beta = \cos(\beta\Theta_a)$. The bare parameters are

$$\Delta v_c = \frac{a_0}{\pi} \left(\frac{3U}{2} - \frac{J_t}{4} \right),$$

$$\Delta v_s = -\frac{a_0}{\pi} \left(\frac{U}{2} - \frac{J_H}{4} + \frac{J_t}{4} \right),$$

$$\Delta v_f = -\frac{a_0}{\pi} \left(\frac{U}{2} - \frac{3J_t}{4} \right),$$

$$\Delta v_{sf} = -\frac{a_0}{\pi} \left(\frac{U}{2} + \frac{J_H}{4} + \frac{J_t}{4} \right),$$

$$A_1 = -\frac{J_H a_0}{4\pi^2},$$

$$A_2 = -\frac{J_H a_0}{2\pi^2},$$

$$A_3 = \frac{a_0}{\pi^2} \left(U - \frac{J_H}{4} - \frac{J_t}{2} \right),$$

$$A_4 = \frac{a_0}{\pi^2} \left(U + \frac{J_t}{2} \right),$$

$$A_5 = \frac{a_0}{\pi^2} \left(U + \frac{J_H}{4} - \frac{J_t}{2} \right). \quad (\text{A6})$$

Finally, the umklapp part of the Hamiltonian reads

$$\mathcal{H}_{\text{umklapp}} = A_6 C_c^{\sqrt{4\pi}} C_s^{\sqrt{4\pi}} + A_7 C_c^{\sqrt{4\pi}} C_f^{\sqrt{4\pi}} + A_8 C_c^{\sqrt{4\pi}} C_{sf}^{\sqrt{4\pi}} + A_9 C_c^{\sqrt{4\pi}} \tilde{C}_{sf}^{\sqrt{4\pi}} \quad (\text{A7})$$

with

$$\begin{aligned} A_6 &= \frac{a_0}{\pi^2} \left(-U - \frac{J_H}{4} + \frac{J_t}{2} \right), \\ A_7 &= \frac{a_0}{\pi^2} \left(-U - \frac{J_t}{2} \right), \\ A_8 &= \frac{a_0}{\pi^2} \left(-U + \frac{J_H}{4} + \frac{J_t}{2} \right), \\ A_9 &= A_2 = -\frac{J_H a_0}{2\pi^2}. \end{aligned} \quad (\text{A8})$$

In the end, a refermionization procedure will allow us to make the exact $U(1)_c \times SU(2)_s \times U(1)_o \times Z_2$ continuous symmetry explicit in the effective Hamiltonian. For this purpose, we introduce eight left- and right-moving Majorana fermions through

$$\begin{aligned} \xi_L^2 + i\xi_L^1 &= \frac{\eta_1}{\sqrt{\pi a_0}} \exp(-i\sqrt{4\pi}\Phi_{sL}), \\ \xi_R^2 + i\xi_R^1 &= \frac{\eta_1}{\sqrt{\pi a_0}} \exp(i\sqrt{4\pi}\Phi_{sR}), \\ \xi_L^4 - i\xi_L^5 &= \frac{\eta_2}{\sqrt{\pi a_0}} \exp(-i\sqrt{4\pi}\Phi_{fL}), \\ \xi_R^4 - i\xi_R^5 &= \frac{\eta_2}{\sqrt{\pi a_0}} \exp(i\sqrt{4\pi}\Phi_{fR}), \\ \xi_L^6 + i\xi_L^3 &= \frac{\eta_3}{\sqrt{\pi a_0}} \exp(-i\sqrt{4\pi}\Phi_{sfL}), \\ \xi_R^6 + i\xi_R^3 &= \frac{\eta_3}{\sqrt{\pi a_0}} \exp(i\sqrt{4\pi}\Phi_{sfR}), \\ \xi_L^8 + i\xi_L^7 &= \frac{\eta_4}{\sqrt{\pi a_0}} \exp(-i\sqrt{4\pi}\Phi_{cL}), \\ \xi_R^8 + i\xi_R^7 &= \frac{\eta_4}{\sqrt{\pi a_0}} \exp(i\sqrt{4\pi}\Phi_{cR}), \end{aligned} \quad (\text{A9})$$

where $\eta_{1,2,3,4}$ are again Klein factors which ensure the adequate anticommutation rules for the fermions. Using this correspondence rules, Eqs. (A4), (A5), and (A7) can be expressed in terms of these eight Majorana fermions. We thus finally obtain the low-energy effective theory for the generalized Hund model (1) at half filling,

$$\begin{aligned} \mathcal{H} &= -\frac{iv_c}{2} \sum_{a=7}^8 (\xi_R^a \partial_x \xi_R^a - \xi_L^a \partial_x \xi_L^a) - \frac{iv_s}{2} \sum_{a=1}^3 (\xi_R^a \partial_x \xi_R^a - \xi_L^a \partial_x \xi_L^a) \\ &\quad - \frac{iv_t}{2} \sum_{a=4}^5 (\xi_R^a \partial_x \xi_R^a - \xi_L^a \partial_x \xi_L^a) - \frac{iv_0}{2} (\xi_R^6 \partial_x \xi_R^6 - \xi_L^6 \partial_x \xi_L^6) \\ &\quad + \frac{g_1}{2} \left(\sum_{a=1}^3 \xi_R^a \xi_L^a \right)^2 + g_2 \left(\sum_{a=1}^3 \xi_R^a \xi_L^a \right) \left(\sum_{a=4}^5 \xi_R^a \xi_L^a \right) \\ &\quad + \xi_R^6 \xi_L^6 \left[g_3 \sum_{a=1}^3 \xi_R^a \xi_L^a + g_4 \sum_{a=4}^5 \xi_R^a \xi_L^a \right] + \frac{g_5}{2} \left(\sum_{a=4}^5 \xi_R^a \xi_L^a \right)^2 \\ &\quad + \frac{g_6}{2} \left(\sum_{a=7}^8 \xi_R^a \xi_L^a \right)^2 + (\xi_R^7 \xi_L^7 + \xi_R^8 \xi_L^8) \times \left[g_7 \sum_{a=1}^3 \xi_R^a \xi_L^a \right. \\ &\quad \left. + g_8 \sum_{a=4}^5 \xi_R^a \xi_L^a + g_9 \xi_R^6 \xi_L^6 \right], \end{aligned} \quad (\text{A10})$$

where the different velocities and couplings are given by

$$\begin{aligned} v_c &= v_F + \frac{a_0}{\pi} \left(\frac{3}{2}U - \frac{J_t}{4} \right), \\ v_s &= v_F - \frac{a_0}{2\pi} \left(U - \frac{J_H}{2} + \frac{J_t}{2} \right), \\ v_t &= v_F - \frac{a_0}{2\pi} \left(U - \frac{3J_t}{2} \right), \\ v_0 &= v_F - \frac{a_0}{2\pi} \left(U + \frac{3J_H}{2} + \frac{J_t}{2} \right), \\ g_1 &= -a_0 \left(U - \frac{J_H}{2} + \frac{J_t}{2} \right), \\ g_2 &= -a_0 \left(U - \frac{J_H}{4} - \frac{J_t}{2} \right), \\ g_3 &= -a_0 \left(U + \frac{J_H}{2} + \frac{J_t}{2} \right), \\ g_4 &= -a_0 \left(U + \frac{3J_H}{4} - \frac{J_t}{2} \right), \\ g_5 &= -a_0 \left(U - \frac{3J_t}{2} \right), \\ g_6 &= a_0 \left(3U - \frac{J_t}{2} \right), \\ g_7 &= a_0 \left(U + \frac{J_H}{4} - \frac{J_t}{2} \right), \\ g_8 &= a_0 \left(U + \frac{J_t}{2} \right), \end{aligned}$$

$$g_9 = a_0 \left(U - \frac{3J_H}{4} - \frac{J_t}{2} \right). \quad (\text{A11})$$

APPENDIX B: EDGE STATES

In this appendix, we investigate the possible existence of edge states in the nondegenerate gapful phases Haldane charge, orbital and spin, when open-boundary conditions are used. The nature of the edge states will reinforce our characterization of, respectively, the HC, HO, and RT phases as being pseudospin-1 chains in, respectively, the charge, orbital, and spin degrees of freedom. Since the occurrence of edge states in the RT phase has already been discussed at length in Ref. 66, we restrict our attention in the following to the HC and HO phases.

1. Open-boundary formalism

The OBC are taken into account by introducing two fictitious sites 0 and $N+1$ in Eq. (1) and by imposing vanishing boundary conditions on the fermion operators: $c_0 = c_{N+1} = 0$.^{78–80} The resulting boundary conditions on the Dirac fermionic fields of Eq. (16) are thus

$$L_{l\sigma}(0) = -R_{l\sigma}(0),$$

$$L_{l\sigma}(x=L) = -(-1)^{L/a_0} R_{l\sigma}(x=L), \quad (\text{B1})$$

with $L = (N+1)a_0$ and $l=1, 2$, $\sigma = \uparrow, \downarrow$. The left- and right-moving Dirac fermions are no longer independent due to the presence of these open boundaries. Using the bosonization formula (A1), we deduce the boundary conditions on the chiral bosonic fields,

$$\Phi_{l\sigma L}(0) = -\Phi_{l\sigma R}(0) + \frac{\sqrt{\pi}}{2} + \sqrt{\pi} p_{l\sigma},$$

$$\Phi_{l\sigma L}(x=L) = -\Phi_{l\sigma R}(x=L) + \frac{\sqrt{\pi}}{2} \left(\frac{L}{a_0} - 1 \right) + \sqrt{\pi} q_{l\sigma}, \quad (\text{B2})$$

where $p_{l\sigma}$ and $q_{l\sigma}$ are integers. The total bosonic field $\Phi_{l\sigma}$ with internal degrees of freedom $l\sigma$ thus obeys Dirichlet boundary conditions,

$$\Phi_{l\sigma}(0) = \frac{\sqrt{\pi}}{2} + \sqrt{\pi} p_{l\sigma},$$

$$\Phi_{l\sigma}(x=L) = \frac{\sqrt{\pi}}{2} \left(\frac{L}{a_0} - 1 \right) + \sqrt{\pi} q_{l\sigma}. \quad (\text{B3})$$

The next step of the approach is to introduce the mode decomposition of the bosonic field $\Phi_{l\sigma}$ compatible with these boundary conditions,

$$\Phi_{l\sigma}(x,t) = \frac{\sqrt{\pi}}{2} + \frac{x}{L} \left[\frac{\sqrt{\pi}}{2} \left(\frac{L}{a_0} - 2 \right) + \tilde{\Pi}_{0l\sigma} \right] + \sum_{n=1}^{\infty} \frac{\sin(n\pi x/L)}{\sqrt{n\pi}} [a_{nl\sigma} e^{-in\pi v_F t/L} + \text{H.c.}], \quad (\text{B4})$$

where $\tilde{\Pi}_{0l\sigma}$ is the zero-mode operator with spectrum $\sqrt{\pi} q_{l\sigma}$ and $a_{nl\sigma}$ is the boson annihilation operator obeying: $[a_{nl\sigma}, a_{m'l'\sigma'}^\dagger] = \delta_{n,m} \delta_{l\sigma, l'\sigma'}$. The mode decomposition of the dual field $\Theta_{l\sigma}$ can then be obtained from the property: $\partial_t \Theta_{l\sigma} = v_F \partial_x \Phi_{l\sigma}$,

$$\Theta_{l\sigma}(x,t) = \tilde{\Phi}_{0l\sigma} + \frac{v_F t}{L} \left[\frac{\sqrt{\pi}}{2} \left(\frac{L}{a_0} - 2 \right) + \tilde{\Pi}_{0l\sigma} \right] + i \sum_{n=1}^{\infty} \frac{\cos(n\pi x/L)}{\sqrt{n\pi}} [a_{nl\sigma} e^{-in\pi v_F t/L} - \text{H.c.}] \quad (\text{B5})$$

with $[\tilde{\Phi}_{0l\sigma}, \tilde{\Pi}_{0l'\sigma'}] = i \delta_{l\sigma, l'\sigma'}$. In particular, $\Phi_{l\sigma}$ and $\Pi_{l\sigma} = \partial_x \Theta_{l\sigma}$ satisfy the equal-time canonical commutation relation for bosons: $[\Phi_{l\sigma}(t,x), \Pi_{l'\sigma'}(t,y)] = i \delta_{l\sigma, l'\sigma'} \delta_L(x-y)$, $\delta_L(x)$ being the delta function at finite size: $\delta_L(x) = \sum_n e^{in\pi x/L} / 2L$. Using the definitions $\Phi_{l\sigma R,L} = (\Phi_{l\sigma} \pm \Theta_{l\sigma})/2$, the mode decomposition of the chiral bosonic fields $\Phi_{l\sigma R,L}$ can then be deduced from Eqs. (B4) and (B5). One can then show that these chiral fields satisfy the following commutation relations when $L \gg a_0$:

$$[\Phi_{l\sigma R,L}(x), \Phi_{l'\sigma' R,L}(y)] = \mp \frac{i}{4} \delta_{l\sigma, l'\sigma'} \text{sgn}(x-y),$$

$$[\Phi_{l\sigma R}(x), \Phi_{l'\sigma' L}(y)] = -\frac{i}{4} \delta_{l\sigma, l'\sigma'} \quad 0 < x, y < L, \quad (\text{B6})$$

$\text{sgn}(x)$ being the sign function. At this point, one should note a technical subtlety which will play its role in the investigation of the possible edge states of the Haldane phases. When considering OBC, the sign of the commutator between $[\Phi_{l\sigma R}, \Phi_{l'\sigma' L}]$ is the opposite of the bulk one [Eq. (A2)]. The latter comes from the identity often used in the bosonization approach,³

$$\Phi_{l\sigma R,L}(x) = \frac{1}{2} \left[\Phi_{l\sigma}(x) \mp \int_{-\infty}^x dy \Pi_{l\sigma}(y) \right], \quad (\text{B7})$$

which does not take properly into account the boundary conditions on the fields. This subtlety has no effect on the derivation of the low-energy Hamiltonian (19) which is still valid in presence of OBC as it can be easily shown. However, it will be important for the discussion of edge states as first observed in Ref. 66 for the determination of boundary excitations of the semi-infinite two-leg spin ladder.

With this formalism at hands, we are now in position to investigate the possible edge states in the generalized Hund model (1) with OBC. To simplify the discussion, we will consider a semi-infinite geometry where the OBC is located at the $i=0$ site and $L \rightarrow +\infty$. The low-energy effective Hamiltonian density is still given by Eq. (19), but now we see,

using the bosonic boundary conditions [Eq. (B2)], the change in basis [Eq. (A3)], and the re-fermionization [Eq. (A9)], that the eight Majorana fermions $\xi_{R,L}^A$ ($A=1, \dots, 8$) must verify the following boundary conditions,

$$\xi_L^A(0) = \xi_R^A(0). \quad (\text{B8})$$

2. Edge states in the Haldane charge phase

Let us set our investigation on the symmetry line $J_H = -8U/3$ where the charge degrees of freedom display an extended SU(2) symmetry and form the pseudospin-1 in charge. For strong attractive U , we expect that the spin and orbital gaps will be larger than the charge gap. This is confirmed numerically by DMRG calculations, for instance, for $U/t = -3$ and $J_t = 0$, the spin and orbital gaps are close respectively to $6t$ and $5t$ while the charge gap is roughly $0.1t$. Within this hypothesis, we can safely integrate out spin and orbital degrees of freedom of model (19). For simplicity, let us choose to work on the line $J_t = J_H/4$, where the spin and orbital degrees of freedom are unified. Keeping only the relevant terms and again neglecting velocity anisotropy, the resulting effective Hamiltonian then reads

$$\mathcal{H} = -\frac{iv_c}{2} \sum_{a=6}^8 \int_0^\infty dx (\xi_{R^a}^a \partial_x \xi_{R^a}^a - \xi_{L^a}^a \partial_x \xi_{L^a}^a) - im_c \int_0^\infty dx \sum_{a=6}^8 \xi_{R^a}^a \xi_{L^a}^a \quad (\text{B9})$$

with the mass m_c given by ($g_7 = g_3$ on the line $J_H = -8U/3$),

$$m_c = ig_7 \sum_{a=1}^5 \langle \xi_{R^a}^a \xi_{L^a}^a \rangle. \quad (\text{B10})$$

Model (B9) is the sum of three decoupled semi-infinite free massive Majorana fermion models. Hence, let us now consider a single Majorana fermion $\xi_{R,L}$ model,

$$\mathcal{H}_m = -\frac{iv}{2} \int_0^\infty dx (\xi_R \partial_x \xi_R - \xi_L \partial_x \xi_L) - im \int_0^\infty dx \xi_R \xi_L \quad (\text{B11})$$

with boundary condition: $\xi_L(0) = \xi_R(0)$. Model (B11) is quadratic with dispersion relation $\epsilon_k = \sqrt{v^2 k^2 + m^2}$ and with the fermionic decomposition⁶⁶

$$\begin{aligned} \xi_R(x, t) &= \frac{1}{\sqrt{2L}} \sum_{k>0} \{ \xi_k [\cos(kx + \theta_k) + i \sin(kx)] e^{-i\epsilon_k t} + \text{H.c.} \} \\ &\quad + \sqrt{\frac{m}{v}} \theta(m) e^{-mx/v} \eta, \\ \xi_L(x, t) &= \frac{1}{\sqrt{2L}} \sum_{k>0} \{ \xi_k [\cos(kx + \theta_k) - i \sin(kx)] e^{-i\epsilon_k t} + \text{H.c.} \} \\ &\quad + \sqrt{\frac{m}{v}} \theta(m) e^{-mx/v} \eta, \end{aligned} \quad (\text{B12})$$

where ξ_k is fermion annihilation operator with wave vector k , θ is the step function, and η is a zero-mode real fermion

normalized according to $\eta^2 = \frac{1}{2}$. In Eq. (B12), θ_k is defined by

$$\exp(i\theta_k) = \frac{vk + im}{\epsilon_k}. \quad (\text{B13})$$

The key point of Eq. (B12) is the existence of an exponentially localized Majorana state with zero energy inside the gap (midgap state) for a positive mass m . In contrast, for negative m , such a zero-mode contribution does not occur since it is not a normalizable solution.

The presence of edge states for the HC phase thus depends on the sign of the mass m_c . Using definition (A9) and commutator (B6), we find

$$m_c = -\frac{g_7}{\pi a_0} \left\langle C_s^{\sqrt{4\pi}} + C_f^{\sqrt{4\pi}} + \frac{1}{2} (C_{sf}^{\sqrt{4\pi}} + \tilde{C}_{sf}^{\sqrt{4\pi}}) \right\rangle. \quad (\text{B14})$$

In the HC phase, we have $\langle \Phi_s \rangle = \langle \Phi_f \rangle = \langle \Theta_{sf} \rangle = 0$ (see Table II) so that $m_c = -5g_7/2\pi$. Hence, since $g_7 = a_0 U$, the mass $m_c > 0$, which signals the emergence of three localized Majorana modes η^a ($a=6, 7, 8$) from the mode decomposition (B12). Moreover, three local Majorana fermion modes are known to define to a local pseudospin- $\frac{1}{2}$ operator \mathcal{J}^a thanks to the identity⁸¹

$$\mathcal{J}^a = -\frac{i}{2} \epsilon^{abc} \eta^{5+b} \eta^{5+c}, \quad (\text{B15})$$

that is a consequence of the anticommutation relations $\{\eta^a, \eta^b\} = \delta^{ab}$. We thus conclude on the existence, in the HC phase, of a pseudospin- $\frac{1}{2}$ edge state at the boundary which can be viewed as a holon edge state.

One recognizes that the pseudospin projection along $\mathcal{J}^1 = -i\eta^7 \eta^8$ is proportional to the total charge generating $U(1)_c$: in the continuum limit, within the convention (A9), one has⁶⁶ $Q_c = \frac{1}{2} \sum_i n_i \rightarrow -i \int dx (\xi_R^7 \xi_R^8 + \xi_L^7 \xi_L^8) = \mathcal{J}^1 - 2i \sum_{k>0} (\xi_k^7 \xi_k^8 - \xi_k^8 \xi_k^7)$, showing that the zero-mode contributes the total charge. In a finite-size system of size L with two boundaries, the edge states come into pairs, which organize into a pseudospin singlet and a pseudospin triplet. Edge states at the two end of the chain interact, leading to a singlet/triplet splitting that goes to zero in the thermodynamical limit. It results that one observes a midgap state with quantum numbers $(Q_c, S^z, T^z) = (L \pm 1, 0, 0)$.

3. Edge states in the Haldane orbital phase

Let us now sit on the symmetry line $J_t = -3J_H/4$ where it is the orbital degrees of freedom that display an extended SU(2) symmetry and form a pseudospin 1. For the sake of simplicity, let us choose to look at line $J_H = 8U$ when charge and spin degrees of freedom are unified into an SO(5) symmetry. For repulsive U , we expect that the charge and spin gap will be higher than the orbital gap (which is confirmed numerically by DMRG simulations, for instance, for $U/t = 1$: the charge and spin gaps are both equal to $6.4t$ while the orbital gap is $0.08t$) so that we can safely integrate out the corresponding degrees of freedom. The resulting leading effective Hamiltonian is (neglecting velocity anisotropy),

$$\mathcal{H} = -\frac{iv_{\perp}}{2} \sum_{a=4}^6 \int_0^{\infty} dx (\xi_R^a \partial_x \xi_R^a - \xi_L^a \partial_x \xi_L^a) - im_o \int_0^{\infty} dx \sum_{a=4}^6 \xi_R^a \xi_L^a \quad (\text{B16})$$

with the mass m_o given by

$$m_o = ig_8 \sum_{a=1}^5 \langle \xi_R^a \xi_L^a \rangle. \quad (\text{B17})$$

The latter mass can be expressed in terms of the ground-state expectation value of the bosonic fields for the charge and spin degrees of freedom,

$$m_o = -\frac{g_8}{\pi a_0} \left\langle C_c^{\sqrt{4\pi}} + C_s^{\sqrt{4\pi}} + \frac{1}{2} (C_{sf}^{\sqrt{4\pi}} + \tilde{C}_{sf}^{\sqrt{4\pi}}) \right\rangle \quad (\text{B18})$$

so that $m_c = -5g_8/2\pi$ in the HO phase (see Table II). As on the considered line, $g_8 = -2a_0U$, the mass $m_o > 0$. We thus conclude on the existence of three localized Majorana modes which form a pseudospin- $\frac{1}{2}$ (orbital) edge state at the boundary in the HO phase.

Repeating the same argument as in the HC phase leads to the expectation—in a finite geometry with size L and two OBC—of a midgap state with quantum numbers $(Q_c, S^z, T^z) = (L, 0, \pm 1)$.

APPENDIX C: STRONG COUPLING AROUND THE ORBITAL LINE

In this appendix, we give a description of the effect of an interchain hopping t_{\perp} in the strong-coupling regime. We will first show that close to the orbital symmetric line ($J_t = -3J_H/4$), a low-energy effective continuous theory can be derived and trivially solved, allowing for the identification of the phases and the phase transitions. Then, we will show that a $U(1)$ symmetry emerges at low energy, similarly to what is known at weak coupling (see Sec. III D).

1. Continuous theory

The effect of the interleg hopping in the strong-coupling regime is in general a complicated problem since the hopping term breaks the $U(1)$ orbital symmetry, this process will induce transitions among on-site states (depicted in Fig. 1) that belong to different symmetry multiplets.

However, as noticed in Sec. II B, for a special fine tuning of the couplings $J_t = -3J_H/4$ the lattice model enjoys a $SU(2)$ symmetry in the orbital sector. Close to this line, the orbital symmetric line, a strong coupling expansion can be performed: orbital degrees of freedom are the only low-energy modes, and an effective Hamiltonian for the orbital operators T^a can be derived, that governs their dynamics. Noticing that the interchain hopping term can be expressed in terms of orbital degrees of freedom, $t_{\perp} \sum_{\sigma,i} (c_{1\sigma,i}^{\dagger} c_{2\sigma,i} + c_{2\sigma,i}^{\dagger} c_{1\sigma,i}) = 2t_{\perp} \sum_i T_i^x$, one remarks that the effect of t_{\perp} close to the $SU(2)_o$ line amounts to the analog of a transverse magnetic field in direction x for orbital degrees of freedom, resulting in the following effective Hamiltonian:

$$\mathcal{H}_{\text{eff}} = J_o \sum_i \vec{T}_i \cdot \vec{T}_{i+1} + D_o \sum_i (T_i^z)^2 + h_o \sum_i T_i^x, \quad (\text{C1})$$

where $J_o = 16t^2/(9J_H + 8U)$, $D_o = J_t + 3J_H/4$, and $h_o = 2t_{\perp}$. Orbital operators T_i being spin-1 operators, close to the orbital line the problem is thus equivalent to a spin-1 Heisenberg model with single-ion anisotropy under a transverse magnetic field.

In the absence of a magnetic field h_o , it is known that the spin-1 Heisenberg chain with a single-ion anisotropy can be described in terms of continuous degrees of freedom, namely, three Majorana fermions⁸² (to be consistent with the main text, we call them ξ^a , $a=4,5,6$), that are related as follows to the uniform components of the spin operators: $T_i^a \rightarrow T^a(x) = i \frac{\epsilon^{abc}}{2} (\xi_L^{3+b} \xi_L^{3+c} + \xi_R^{3+b} \xi_R^{3+c}) + \dots$, where the dots indicate oscillating terms. The low-energy spectrum of the theory is well described, at lowest order, by a theory of three free massive fermions, corresponding to three branches of magnons. Now the magnetic field also yields a term that is quadratic in fermions. Neglecting velocity anisotropies, we thus end up with the following quadratic Hamiltonian:

$$\mathcal{H}_{\text{cont}} = -\frac{iv_o}{2} \sum_{a=4}^6 (\xi_R^a \partial_x \xi_R^a - \xi_L^a \partial_x \xi_L^a) + i \sum_a m_a \xi_R^a \xi_L^a + ih_o (\xi_L^5 \xi_L^6 + \xi_R^5 \xi_R^6). \quad (\text{C2})$$

The masses m_a are phenomenological parameters. When $D_o = t_{\perp} = 0$, one has a single mass scale $m \propto J_o$ (the gap of the spin-1 Heisenberg chain), and in the general case one can parametrize them as $m_4 = m_5 = m - \delta$ and $m_6 = m + \delta$, with $\delta \propto D_o$ at first order in D_o/J_o . One immediately sees that the fermion ξ^4 decouples. Fourier transforming the remaining fermions, $\xi_{L(R)}^a(k) = \int dx e^{-ikx} \xi_{L(R)}^a(x)$, and introducing $\Psi_k = [\xi_L^5(k), \xi_R^5(k), \xi_L^6(k), \xi_R^6(k)]$ the Hamiltonian reads $\sum_{k>0} \Psi_{-k} U_k \Psi_k$. The one-particle spectrum is obtained from the eigenvalues of the matrix,

$$U_k = \begin{pmatrix} v_o k & im_5 & ih_o & 0 \\ -im_5 & -v_o k & 0 & ih_o \\ -ih_o & 0 & v_o k & im_6 \\ 0 & -ih_o & -im_6 & -v_o k \end{pmatrix}. \quad (\text{C3})$$

This yields two branches with energies: $\epsilon_{\pm}(k) = \sqrt{\epsilon_0^2(k) + h_o^2 + \delta^2 \pm 2\sqrt{h_o^2 \epsilon_0^2(k) + m^2 \delta^2}}$, where $\epsilon_0(k)$ is the spectrum at $D_o = t_{\perp} = 0$: $\epsilon_0(k) = \sqrt{v_o^2 k^2 + m^2}$.

We can now identify several phase transition lines, for which the spectrum is massless, i.e., admits modes of arbitrary low energy. A first Ising transition line is readily obtained when $\delta = m$: then $m_4 = 0$.

Other critical lines are found by solving the equation $\epsilon_{-}(k^*) = 0$ [the branch $\epsilon_{+}(k)$ is always gapful]: one finds that for $h_o^2 + \delta^2 = m^2$, this equation has a solution $k^* = 0$, and for $\delta = 0$ and $|h_o| > m$, two solutions $k^* = \pm |k^*| \neq 0$, with $v_o^2 k^{*2} = h_o^2 - m^2$. On the former critical line, the massless degrees of freedom consist in a single Majorana mode and one has a central charge $c = \frac{1}{2}$. The latter critical line has central charge

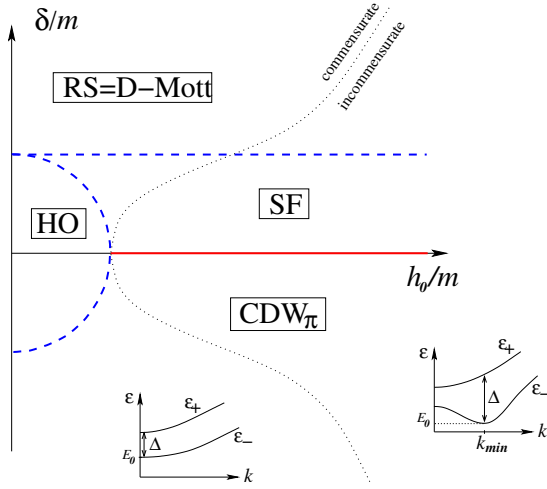


FIG. 14. (Color online) Phase diagram of the generalized Hund ladder with interchain hopping. The coordinate on the horizontal axis is proportional to t_{\perp} whereas that on the vertical axis is the distance D_o to the SU(2) orbital symmetric model. Bold (blue) dashed lines indicate $c=\frac{1}{2}$ critical lines, while the bold (red) one is a $c=1$ critical line. See the main text for the definition of the phases. The dotted line, with equation $m^2\delta^2=h_o^2(h_o^2-m^2)$, indicates the location where incommensuration appears: on the right of this curve, the lower band ϵ_- displays a minimum for a wave vector k_{min} . The two insets display the typical spectrum in the commensurate and incommensurate regions, respectively.

$c=1$, and corresponds to the well-known commensurate/incommensurate transition of the isotropic spin-1 Heisenberg chain under a magnetic field.

To identify the phases of the ladder lying on both sides of those lines (see Fig. 14), one notices that by continuity with what happens at $t_{\perp}=0$, the phase with $m_4 < 0$ (obtained at large enough δ) must be a RS phase (which coincides with the D-Mott phase). The phase at $m_4 > 0$ is readily identified by means of the duality transformation $\xi_L^A \rightarrow -\xi_L^A$ that amounts to $\Phi_f \leftrightarrow \sqrt{\pi}/2 - \Theta_f$ [see Eq. (A9)]: it is a SF phase.

By continuity with $t_{\perp}=0$, the pocket $\delta^2+h_o^2 < m^2$ corresponds to a HO phase. The last phase to be mapped out is the one lying at $h_o^2+\delta^2 > m^2$ and $\delta < 0$: it is adiabatically connected to the ODW phase that one has obtained at $t_{\perp}=0$ and $D_o < 0$ so that it is an ODW or CDW $_{\pi}$ phase, as we named it in the context of the ladder with an interchain hopping.

2. Effective low-energy theory

We now make a qualitative connection with the weak-coupling analysis of Sec. III D, which crucially relies on the existence of an extended $U(1)$ symmetry in the orbital sector, and show that this symmetry is also emergent at low energy in the strong-coupling regime. In the strong-coupling limit, in the vicinity of the orbital symmetric line, the interchain hopping t_{\perp} amounts to a magnetic field in orbital space, that will eventually drive the system to a incommensurate state: when $\delta=0$, as soon as $h_o > m$ the Fermi points shift to $k_F = \frac{\pi}{2a_0} + k^*$. Now if the “magnetic field” is large enough, i.e., if k^* is large enough, this leaves the space for a low-energy

description built on fields expanded around the new Fermi points. In this effective low-energy description, $4k_F$ umklapp terms have no effect as being strongly oscillating. This remains true if one departs from the orbital symmetric line $\delta=0$: in this case, the spectrum of the low-energy band, $\epsilon_-(k)$, develops a gap but the incommensuration is still present in the form of a minimum (which becomes infinitely deep in the limit $h_o \gg m$) in $\epsilon_-(k)$ at a value $v_o k_{min} = \sqrt{h_o^2 - m^2} (1 + \frac{\delta^2}{h_o^2})$. This happens (see Fig. 14) when δ is small enough, $|\delta| < \delta_c = h_o \sqrt{\frac{h_o^2}{m^2} - 1}$. But is there an associated emergent symmetry, as it was the case in the weak-coupling limit?

To investigate this, one has to enter into further details. Denoting by A_k the unitary matrix diagonalizing U_k , with $A_k^\dagger U_k A_k = \text{diag}[\epsilon_-(k), -\epsilon_-(k), \epsilon_+(k), -\epsilon_+(k)]$, and introducing $\tilde{\Psi}_k = A_k^{-1} \Psi_k = [\chi_-(k), \chi_+(k)]$, one can represent in the eigenmode basis the orbital U(1) generators along x , $T_{tot,\pm}^x = i \int dx (\xi_L^5 \xi_L^6 \pm \xi_R^5 \xi_R^6) = \int_{k>0} \tilde{\Psi}_k^\dagger T_k^{(\pm)} \tilde{\Psi}_k$. $T_{tot,\pm}^x$ are the total Noether charge and current. The Hermitian matrix elements $T_{k,\alpha\beta}^{(\pm)}$ are too cumbersome, and not particularly enlightening, to appear here, but the matrix $T_k^{(-)}$ has a remarkable block structure,

$$T_k^{(-)} = \begin{pmatrix} t_1(k)\mathbb{I} & t_2(k)\sigma^z + t_3(k)\sigma^x \\ t_2(k)\sigma^z + t_3(k)\sigma^x & -t_1(k)\mathbb{I} \end{pmatrix}. \quad (C4)$$

Let us now introduce two quantities characterizing the spectrum: the absolute minimum E_0 of the lower band, and the gap Δ from the minimum of the lower band E_0 to the upper band (see insets of Fig. 14). Now, if the two bands $\epsilon_+(k)$ and $\epsilon_-(k)$ are well separated, i.e., if $\Delta \gg E_0$, it makes sense to describe the theory at low energies in terms of the two Majorana fermions $\chi_-(k)$. Introducing the projector P^- that projects on this subspace, the effective Hamiltonian $H_{\text{eff}}^- = P^- H P^- = \sum_k \epsilon_-(k) \chi_-^\dagger(k) \sigma_z \chi_-(k)$ commutes with $P^- T_{tot,-}^x P^-$. Thus, the total orbital current along x is asymptotically conserved in the limit of large Δ/E_0 , and the low-energy theory is effectively $U(1)$ symmetric. For a physical quantity computed in the low-energy, $U(1)$ -symmetric theory, violation of this emergent symmetry by processes connecting the two bands will result in corrections of order $(E_0/\Delta)^2$.

Now, the parameters E_0 and Δ bear qualitatively distinct forms in the commensurate and incommensurate regions. For simplicity, we restrict our attention to the case $h_o > m$. In the commensurate region, one has

$$E_0 = \sqrt{\delta^2 + h_o^2} - m, \quad \Delta = 2m \quad (C5)$$

so that in general E_0/Δ is not small.

In contrast, in the incommensurate region, one has

$$E_0 = \delta \sqrt{1 - \frac{m^2}{h_o^2}} \leq \mathcal{O}(\delta),$$

$$\Delta = \sqrt{4h_o^2 + E_0^2} - E_0 \quad (\text{C6})$$

so that the symmetry $\widetilde{\text{U}}(1)$ is violated by terms of order $(\delta/2h_o)^2$: the symmetry $\text{U}(1)$ is asymptotically exact in the limit $h_o \gg \delta$. One thus concludes that close to the line $J_t = -3J_H/4$, the situation at large coupling coincides with that at small coupling. One can thus reasonably infer that this sym-

metry is emergent in all regimes at least close to the line $J_t = -3J_H/4$. Our strong-coupling analysis suggests that the emergent $\text{U}(1)$ is broken when moving far away from the orbital symmetric line; however, the question of the existence of such an emergent symmetry in the strong-coupling regime of the generic electronic two-leg ladder goes far beyond the scope of this paper.

- ¹S. Sachdev, *Quantum Phase Transitions* (Cambridge University Press, Cambridge, England, 1999).
- ²T. Senthil, A. Vishwanath, L. Balents, S. Sachdev, and M. P. A. Fisher, *Science* **303**, 1490 (2004); T. Senthil, L. Balents, S. Sachdev, A. Vishwanath, and M. P. A. Fisher, *Phys. Rev. B* **70**, 144407 (2004).
- ³A. O. Gogolin, A. A. Nersesyan, and A. M. Tsvelik, *Bosonization and Strongly Correlated Systems* (Cambridge University Press, Cambridge, England, 1998).
- ⁴T. Giamarchi, *Quantum Physics in One Dimension* (Clarendon press, Oxford, UK, 2004).
- ⁵H.-H. Lin, L. Balents, and M. P. A. Fisher, *Phys. Rev. B* **58**, 1794 (1998).
- ⁶D. Scalapino, S.-C. Zhang, and W. Hanke, *Phys. Rev. B* **58**, 443 (1998).
- ⁷H. Frahm and M. Stahlsmeier, *Phys. Rev. B* **63**, 125109 (2001).
- ⁸K. Le Hur, *Phys. Rev. B* **63**, 165110 (2001).
- ⁹J. B. Marston, J. O. Fjærestad, and A. Sudbo, *Phys. Rev. Lett.* **89**, 056404 (2002).
- ¹⁰J. O. Fjærestad and J. B. Marston, *Phys. Rev. B* **65**, 125106 (2002).
- ¹¹M. Tsuchiizu and A. Furusaki, *Phys. Rev. B* **66**, 245106 (2002).
- ¹²C. Wu, W. V. Liu, and E. Fradkin, *Phys. Rev. B* **68**, 115104 (2003).
- ¹³T. Momoi and T. Hikihara, *Phys. Rev. Lett.* **91**, 256405 (2003).
- ¹⁴R. Assaraf, P. Azaria, E. Boulat, M. Caffarel, and P. Lecheminant, *Phys. Rev. Lett.* **93**, 016407 (2004).
- ¹⁵M. Fabrizio and E. Tosatti, *Phys. Rev. Lett.* **94**, 106403 (2005).
- ¹⁶S. Lee, J. B. Marston, and J. O. Fjærestad, *Phys. Rev. B* **72**, 075126 (2005).
- ¹⁷J. O. Fjærestad, J. B. Marston, and U. Schollwöck, *Ann. Phys. (N.Y.)* **321**, 894 (2006).
- ¹⁸J. E. Bunder and H.-H. Lin, *Phys. Rev. B* **79**, 045132 (2009).
- ¹⁹H.-H. Lin, *Phys. Rev. B* **58**, 4963 (1998).
- ²⁰A. A. Nersesyan and A. M. Tsvelik, *Phys. Rev. B* **68**, 235419 (2003).
- ²¹S. T. Carr, A. O. Gogolin, and A. A. Nersesyan, *Phys. Rev. B* **76**, 245121 (2007).
- ²²J. E. Bunder and H.-H. Lin, *Phys. Rev. B* **78**, 035401 (2008).
- ²³F. D. M. Haldane, *Phys. Lett. A* **93**, 464 (1983); *Phys. Rev. Lett.* **50**, 1153 (1983).
- ²⁴T. Kennedy and H. Tasaki, *Phys. Rev. B* **45**, 304 (1992).
- ²⁵D. G. Shelton, A. A. Nersesyan, and A. M. Tsvelik, *Phys. Rev. B* **53**, 8521 (1996); A. A. Nersesyan and A. M. Tsvelik, *Phys. Rev. Lett.* **78**, 3939 (1997); **79**, 1171(E) (1997).
- ²⁶H. Watanabe, *Phys. Rev. B* **52**, 12508 (1995); Y. Nishiyama, N. Hatano, and M. Suzuki, *J. Phys. Soc. Jpn.* **64**, 1967 (1995); S. R. White, *Phys. Rev. B* **53**, 52 (1996).
- ²⁷H. J. Schulz, [arXiv:cond-mat/9808167](https://arxiv.org/abs/cond-mat/9808167) (unpublished).
- ²⁸H. C. Lee, P. Azaria, and E. Boulat, *Phys. Rev. B* **69**, 155109 (2004).
- ²⁹D. Controzzi and A. M. Tsvelik, *Phys. Rev. B* **72**, 035110 (2005).
- ³⁰P. Lecheminant and K. Totsuka, *Phys. Rev. B* **71**, 020407(R) (2005); **74**, 224426 (2006).
- ³¹E. Boulat, P. Azaria, and P. Lecheminant, *Nucl. Phys. B* **822**, 367 (2009).
- ³²D. P. Arovas and A. Auerbach, *Phys. Rev. B* **52**, 10114 (1995).
- ³³T. Fukuhara, Y. Takasu, M. Kumakura, and Y. Takahashi, *Phys. Rev. Lett.* **98**, 030401 (2007); S. Taie, Y. Takasu, S. Sugawa, R. Yamazaki, T. Tsujimoto, R. Murakami, and Y. Takahashi, [arXiv:1005.3670](https://arxiv.org/abs/1005.3670) (unpublished).
- ³⁴A. V. Gorshkov, M. Hermele, V. Gurarie, C. Xu, P. S. Julienne, J. Ye, P. Zoller, E. Demler, M. D. Lukin, and A. M. Rey, *Nat. Phys.* **6**, 289 (2010).
- ³⁵Y. Yamashita, N. Shibata, and K. Ueda, *Phys. Rev. B* **58**, 9114 (1998).
- ³⁶S. K. Pati, R. R. P. Singh, and D. I. Khomskii, *Phys. Rev. Lett.* **81**, 5406 (1998).
- ³⁷B. Frischmuth, F. Mila, and M. Troyer, *Phys. Rev. Lett.* **82**, 835 (1999).
- ³⁸P. Azaria, A. O. Gogolin, P. Lecheminant, and A. A. Nersesyan, *Phys. Rev. Lett.* **83**, 624 (1999); P. Azaria, E. Boulat, and P. Lecheminant, *Phys. Rev. B* **61**, 12112 (2000).
- ³⁹C. Itoi, S. Qin, and I. Affleck, *Phys. Rev. B* **61**, 6747 (2000).
- ⁴⁰C. Wu, J. P. Hu, and S. C. Zhang, *Phys. Rev. Lett.* **91**, 186402 (2003).
- ⁴¹P. Lecheminant, E. Boulat, and P. Azaria, *Phys. Rev. Lett.* **95**, 240402 (2005); P. Lecheminant, P. Azaria, and E. Boulat, *Nucl. Phys. B* **798**, 443 (2008).
- ⁴²C. Wu, *Phys. Rev. Lett.* **95**, 266404 (2005).
- ⁴³D. Controzzi and A. M. Tsvelik, *Phys. Rev. Lett.* **96**, 097205 (2006).
- ⁴⁴H.-H. Tu, G.-M. Zhang, and L. Yu, *Phys. Rev. B* **76**, 014438 (2007); **74**, 174404 (2006).
- ⁴⁵C. J. Wu, *Mod. Phys. Lett. B* **20**, 1707 (2006).
- ⁴⁶S. Capponi, G. Roux, P. Azaria, E. Boulat, and P. Lecheminant, *Phys. Rev. B* **75**, 100503(R) (2007).
- ⁴⁷S. Capponi, G. Roux, P. Lecheminant, P. Azaria, E. Boulat, and S. R. White, *Phys. Rev. A* **77**, 013624 (2008).
- ⁴⁸G. Roux, S. Capponi, P. Lecheminant, and P. Azaria, *Eur. Phys. J. B* **68**, 293 (2009).
- ⁴⁹Y. Jiang, J. Cao, and Y. Wang, *EPL* **87**, 10006 (2009).
- ⁵⁰H. Nonne, P. Lecheminant, S. Capponi, G. Roux, and E. Boulat, *Phys. Rev. B* **81**, 020408(R) (2010).
- ⁵¹R. Assaraf, P. Azaria, M. Caffarel, and P. Lecheminant, *Phys.*

- Rev. B **60**, 2299 (1999).
- ⁵²E. Szirmai, O. Legeza, and J. Solyom, *Phys. Rev. B* **77**, 045106 (2008); K. Buchta, O. Legeza, E. Szirmai, and J. Solyom, *ibid.* **75**, 155108 (2007).
- ⁵³J. Zhao, K. Ueda, and X. Wang, *Phys. Rev. B* **74**, 233102 (2006).
- ⁵⁴S. Capponi, C. J. Wu, and S. C. Zhang, *Phys. Rev. B* **70**, 220505 (2004).
- ⁵⁵S.-C. Zhang, *Science* **275**, 1089 (1997); E. Demler, W. Hanke, and S.-C. Zhang, *Rev. Mod. Phys.* **76**, 909 (2004).
- ⁵⁶S. R. White, *Phys. Rev. Lett.* **69**, 2863 (1992); *Phys. Rev. B* **48**, 10345 (1993); U. Schollwöck, *Rev. Mod. Phys.* **77**, 259 (2005).
- ⁵⁷C. N. Yang, *Phys. Rev. Lett.* **63**, 2144 (1989).
- ⁵⁸C. N. Yang and S. C. Zhang, *Mod. Phys. Lett. B* **4**, 759 (1990); S.-C. Zhang, *Int. J. Mod. Phys. B* **5**, 153 (1991).
- ⁵⁹P. W. Anderson, *Phys. Rev.* **112**, 1900 (1958).
- ⁶⁰I. Affleck, D. P. Arovas, J. B. Marston, and D. A. Rabson, *Nucl. Phys. B* **366**, 467 (1991).
- ⁶¹A. V. Onufriev and J. B. Marston, *Phys. Rev. B* **59**, 12573 (1999).
- ⁶²M. den Nijs and K. Rommelse, *Phys. Rev. B* **40**, 4709 (1989).
- ⁶³E. H. Kim, G. Fáth, J. Sólyom, and D. J. Scalapino, *Phys. Rev. B* **62**, 14965 (2000).
- ⁶⁴I. Affleck, T. Kennedy, E. H. Lieb, and H. Tasaki, *Phys. Rev. Lett.* **59**, 799 (1987); *Commun. Math. Phys.* **115**, 477 (1988).
- ⁶⁵T. Kennedy, *J. Phys.: Condens. Matter* **2**, 5737 (1990).
- ⁶⁶P. Lecheminant and E. Orignac, *Phys. Rev. B* **65**, 174406 (2002).
- ⁶⁷H. J. Schulz, *Phys. Rev. B* **34**, 6372 (1986).
- ⁶⁸P. Di Francesco, P. Mathieu, and D. Sénéchal, *Conformal Field Theory* (Springer, Berlin, 1997).
- ⁶⁹D. Allen and D. Sénéchal, *Phys. Rev. B* **55**, 299 (1997).
- ⁷⁰G. Mussardo, *Statistical Field Theory: An Introduction to Exactly Solved Models in Statistical Physics* (Clarendon press, Oxford, UK, 2009).
- ⁷¹D. J. Gross and A. Neveu, *Phys. Rev. D* **10**, 3235 (1974).
- ⁷²A. B. Zamolodchikov and Al. B. Zamolodchikov, *Ann. Phys. (N.Y.)* **120**, 253 (1979).
- ⁷³F. H. L. Essler and R. M. Konik, in *From Fields to Strings: Circumnavigating Theoretical Physics*, I. Kogan Memorial, edited by M. Shifman, A. Vainshtein, and J. Wheeler (World Scientific, Singapore, 2005).
- ⁷⁴M. Nakamura, *Physica B* **329-333**, 1000 (2003).
- ⁷⁵E. Berg, E. G. Dalla Torre, T. Giamarchi, and E. Altman, *Phys. Rev. B* **77**, 245119 (2008).
- ⁷⁶This phase is equivalent to the ODW phase for $t_{\perp}=0$.
- ⁷⁷This phase is equivalent to the staggered dimerization phase (SP_{π} phase) that we have found for $t_{\perp}=0$.
- ⁷⁸S. Eggert and I. Affleck, *Phys. Rev. B* **46**, 10866 (1992).
- ⁷⁹E. Wong and I. Affleck, *Nucl. Phys. B* **417**, 403 (1994).
- ⁸⁰M. Fabrizio and A. O. Gogolin, *Phys. Rev. B* **51**, 17827 (1995).
- ⁸¹A. M. Tsvelik, *Phys. Rev. Lett.* **69**, 2142 (1992).
- ⁸²A. M. Tsvelik, *Phys. Rev. B* **42**, 10499 (1990).